Response to reviewers

We gratefully thank the reviewer for the constructive comments and suggestions to improve the manuscript. Below are the detailed point-to-point responses to the reviewer's comments. For clarity, the reviewer's comments are listed below in *black italics*, while our responses and changes in the manuscript are shown in blue. The changes in the revised manuscript and supporting materials are also highlighted.

Anonymous Referee #1

Review of Sun et al. 2023: Measurement report: Atmospheric Ice Nuclei at Changbai Mountain (2623 m a.s.l.) in Northeastern Asia

Sun et al. 2023 present INP measurement results from the Changbai mountain in summer 2021. Changes in INP concentration are investigated towards diurnal variability, composition, source, and transport mechanism. It is an interesting study given the location of the measurement site, methodology and efforts taken in the analysis. However, major adjustments are needed to streamline and support the claims of the manuscript.

Response: We are grateful to the reviewer for the comments and have endeavored to respond to these and revise our manuscript accordingly.

General Comments:

Major doubts concern the influence of the PBL height to Changbai mountain in Section 3.4. To the reviewer the analysis and interpretation are inconclusive. Especially it is not entirely traceable how the PBL height was derived and the involved error. Given the points raised below, the reviewer is not entirely sure if some claims need to be removed if not being support by further evidence from in-situ observations. In addition, the local wind system and dynamics should be better described or referenced.

Overall, it appears that frequently there are statements in the manuscript that should be supported by a reference. The authors may want to consider this aspect, while working through the manuscript. In addition, the figures of the manuscript could also be linked to the made statements more often. Furthermore, there appear some side information at some point, which not necessarily add to the flow of the manuscript. The authors may want to critically read through the paper, deciding which information is needed to reach the presented conclusions.

Some strong statements are made without reference or presenting data. For additional support of some of the made claims particle size measurements may be helpful. Have there not measurements been available for the study?

Changbai mountain is referred as 2623 m a.s.l. (Tianchi site) and 2740 m a.s.l. (highest point). To avoid confusion the two locations and heights should be consistently appear combined.

For deeper explanations, see specific comments below.

Response: Thanks for the comment. In this study, the PBL data was obtained from the fifth-generation ECMWF global atmospheric reanalysis (ERA5 reanalysis). The reliability of ERA5 dataset has been substantiated in previous studies, such as Le et al. (2020), Tornow et al. (2021), and Slattberg et al. (2022). We made more specified statements regarding the source and data reliability of the PBL in the following response. Further details regarding the source and the robustness of the PBL data can be found in the subsequent responses.

We calculated the 72-hour backward trajectories, and found that prevailing air masses predominantly approached the sampling site from the east. However, the local winds exhibited a prevailing pattern from the west and south. The Changbai Mountains feature a topography characterized by higher elevations in the southeast and lower elevations in the northwest, and our observation site is located in the northwest direction. We inferred that air masses arriving from the east encounter obstruction by the Changbai Mountains, resulting in a lifting along the southern to western slopes. Combined with the trajectory heights of the air masses, it is evident that as the air mass approached the observation sites, their trajectories inclined upward along the southern or southwestern mountainsides. These findings suggested that the air masses underwent a noticeable lifting process prior to reaching the sampling site, potentially attributed to orographic lifting along the mountain slopes in the south and westward directions. We have added this information into the revised manuscript to provide a clearer understanding of the wind dynamics in this region.

We have added essential references to provide more comprehensive support for some of the statements. Furthermore, we have improved the integration of figure citations within the context. To enhance the overall flow of the article, we have removed the discussion of secondary ice formation from the conclusion section.

We apologize for the absence of parallel size measurements to distinguish particle chemical concentrations between particles larger than 2.5 μm and those smaller than 2.5 μm. This may result in some uncertainties in the investigation of the sources of INPs based on $PM_{2.5}$ chemical composition. These uncertainties have been addressed in the revised manuscript.

Our sampling site is situated at an elevation of 2623 m a.s.l. on Changbai Mountain. Notably, Lu et al. (2016) collected rainwater samples at the peak of Changbai mountain, which stands at an elevation of 2740 m a.s.l. We have clarified this in the revised manuscript.

Moreover, we diluted the untreated and heat-treated samples by the factors of 30, 60, and 120 times, and extended the freezing temperature below -25°C. We have updated the N_{INP} spectra and analysis in the whole revised manuscript.

Detailed point-to-point responses are shown below.

Specific Comments:

Introduction

1. L29: 'As most precipitation in clouds initiates via the ice phase', this statement could be refined in regard of which cloud types and regions are affected and direct studies could be cited.

Response: Thanks for the comment. We have revised this statement as follows: "Global precipitation is predominantly produced by clouds containing the ice phase, especially in continental regions and mid-latitude oceans, emphasizing the paramount significance of investigating ice formation within clouds (Mulmenstadt et al., 2015; Lau and Wu, 2003; Demott et al., 2010; Kanji et al., 2017)."

2. L63: 'At present, it is unclear whether…', in the reviewer's opinion the current knowledge gap is not whether but to which extend and through which transport pathway INPs are brought to MPC relevant heights.

Response: We agree and have therefore revised the statement as follows: "At present, there remain uncertainties how INPs can be extended and transported to the altitudes of mixed-phase cloud formation (approximately 3–7 km)."

3. L68: One station in Conen et al. 2017 was located outside the Swiss Alps.

Response: Thanks for the comment. We have revised the statement as follows: "For example, in the Switzerland, simultaneous measurements taken at different-altitude stations revealed a reduction of approximately 50% per kilometer in the abundance of INPs in the vertical gradient (ranging from 489 m above sea level (a.s.l.) to 3580 m a.s.l. in the Swiss Alps) in the warm season (Conen et al., 2017)."

4. L71: Wieder et al. 2022 sampled frequently for short time spans throughout the day, whereas Conen et al. 2017 used filters sampling over longer timespans. Wieder et al. 2022 observed also a diurnal cycle with INP concentrations seeming to equilibrate over the course of a day. Further it may be important to point out to the reader that this was only observed in a wind direction where the topography promoted vertical transport of air masses from lower elevation.

Response: Thanks for the comment. We have added "Note that variations in sampling methods and the influence of wind directions can also exert an impact on INP concentrations." in the revised manuscript.

5. L75-77: "For example, at the Jungfraujoch station (3580 m a.s.l.) in the Swiss Alps, approximately 80% of INPs were biological aerosols at freezing temperatures above −15 °C" – add reference.

Response: We apologize for missing this reference and cited it in the revised manuscript (Conen et al., 2022).

6. L81-82: "… and establishing a parametric equation that depends on temperature and ice supersaturation for predicting the INPs concentration" – this information seems irrelevant for the current study.

Response: We agree and have removed it in the revised manuscript.

7. L83: Here, Changbai mountain is attributed with a height of 2740 m a.s.l., whereas in L87 a height of 2623 m a.s.l. is given. If understood correct, the latter height refers to the INP measurement station of the current study. To avoid confusion the distinction between the peak and the measurement station should be made (also throughout the manuscript).

Response: Yes, the 2740 m a.s.l. in Line 83 was the peak height of Changbai mountain, and the 2623 m a.s.l. in Line 87 was the height of our sampling site. To avoid confusion, we have revised as "Changbai Mountain (at the peak of 2740 m a.s.l.)".

Methods

8. L102: Shouldn't the elevations around the mountain decrease to all directions?

Response: The elevations gradient around the mountain generally decreases to all directions. However, we aimed to describe the comprehensive pattern of height changes across the entire mountain, which is higher elevation in the southeast compared to the northwest directions. This has been clarified in the revised manuscript.

9. L104: Is 150m correct? Looking at maps it seems like more.

Response: Thanks. We carefully checked the distance from our observation site to Tianchi Lake, and revised the distance to 410 m in the manuscript.

10. L106-112: Adding a timeseries plot (appendix or supplement) of the general meteorological parameters throughout the campaign including exemplary INP concentration would be helpful to understand the sampling conditions.

Response: Figure R1 has been added to the Supporting Information and mentioned in section 2.1 as follows: "Figure S1 presents the timeseries of meteorological parameter, NOx concentration, and the of INP concentrations during the field measurements."

In addition, detailed sampling information has been added in Table S1 in the Supporting Information, as presented in Table R1.

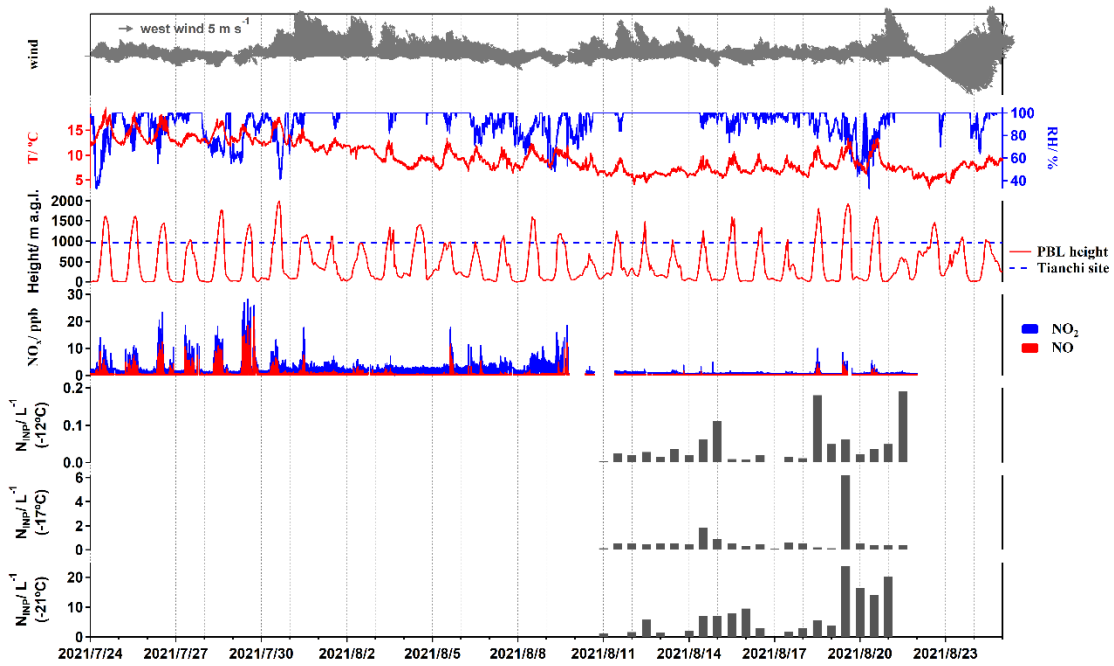

Figure R1. Time series of meteorological parameter (i.e., wind, temperature, and RH), the height of PBL and Tianchi site (above ground level), NO_x and the cumulative number concentration of INPs (N_{INP}) at -12 ℃, -17 ℃ and -21 ℃ measured during the campaign.

Table R1. Detail information including sampling date, duration and total sampling volume in this study.

Sample Date	Start time	End time	Duration/ min	Total Volume/ L
2021.8.10-Night	2021/8/10 18:00	2021/8/11 5:30	294	34500
2021.8.11-Day	2021/8/11 10:30	2021/8/11 17:30	168	21000
2021.8.11-Night	2021/8/11 18:00 2021/8/11 20:32	2021/8/11 20:26 2021/8/12 3:32	242	28300
2021.8.12-Day	2021/8/12 6:00	2021/8/12 17:30	294	34500
2021.8.12-Night	2021/8/12 18:00	2021/8/13 5:30	294	34500
2021.8.13-Day	2021/8/13 6:00	2021/8/13 17:30	294	34500
2021.8.13-Night	2021/8/13 18:00	2021/8/14 5:30	294	34500
2021.8.14-Day	2021/8/14 6:00	2021/8/14 17:30	294	34500
2021.8.14-Night	2021/8/14 18:00	2021/8/15 5:30	294	34500
2021.8.15-Day	2021/8/15 6:00	2021/8/15 18:00	288	36000
2021.8.15-Night	2021/8/15 18:30	2021/8/16 5:30	264	33000
2021.8.16-Day	2021/8/16 6:00	2021/8/16 17:30	294	34500
2021.8.16-Night	2021/8/16 18:00	2021/8/17 5:30	294	34500
2021.8.17-Day	2021/8/17 6:00	2021/8/17 17:30	294	34500
2021.8.17-Night	2021/8/17 18:00	2021/8/18 5:30	294	34500
2021.8.18-Day	2021/8/18 10:00	2021/8/18 17:30	198	22500
2021.8.18-Night	2021/8/18 18:00	2021/8/19 5:30	294	34500
2021.8.19-Day	2021/8/19 6:00	2021/8/19 17:30	294	34500
2021.8.19-Night	2021/8/19 18:00	2021/8/20 5:30	294	34500
2021.8.20-Day	2021/8/20 6:00	2021/8/20 17:30	294	34500
2021.8.20-Night	2021/8/20 18:00	2021/8/21 5:30	294	34500
2021.8.21-Day	2021/8/21 6:00	2021/8/21 17:30	294	34500
Blank-Night	2021/8/23 17:29	2021/8/24 5:36	295	-
Blank-Day	2021/8/24 7:30	2021/8/24 18:50	284	-

11. L112: What about touristic activities?

Response: We have added the touristic activities in the revised manuscript: "Changbai Mountain is a national nature reserve with no large industrial facilities nearby, and tourism is the important economic activity in the region. Due to the emergence of novel coronavirus (COVID-19) cases, strict lockdown measures have been implemented from August 10, 2021, resulting in a substantial reduction in visitor numbers, as indicated by the marked decrease in NOx concentration (Figure S1)."

12. L114: How was differentiated whether the sampling site was in the free troposphere or influenced by the PBL? Please elaborate and add data or reference.

Response: In Figure R1 (and also in Figure S1), we have included PBL data represented by the red line, while the blue dashed line corresponds to the height of the sampling site. Throughout the observation period, the sampling site experiences alternations between the free troposphere and the boundary layer due to changes in the PBL.

13. L116: A dedicated reader may be interested in a picture of the setup (also possibly in the appendix or supplement).

Response: We added the picture of the TH-150D medium flow sampler in Figure 1 in the revised manuscript, as show in Figure R2b.

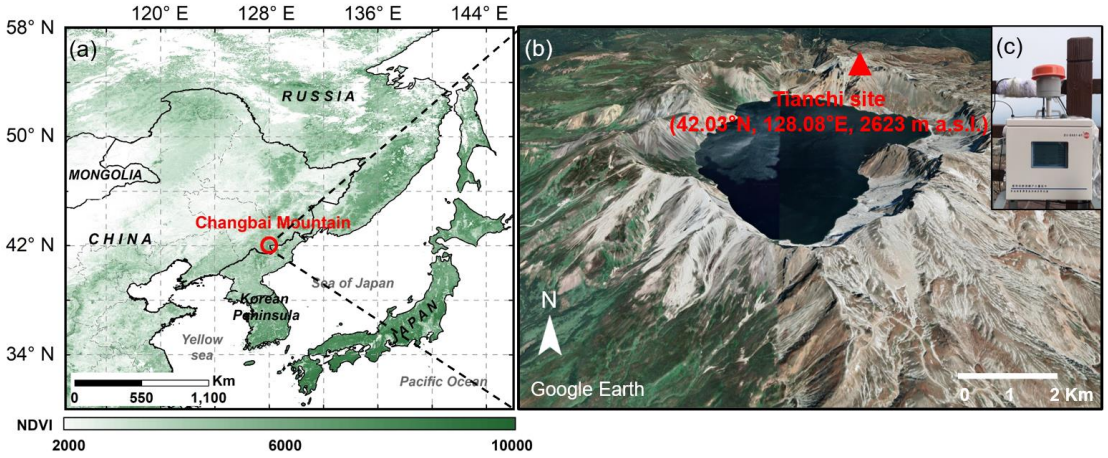

Figure R2. Geographical maps showing the location of Changbai Mountain. (a) This map is color-coded according to the normalized difference vegetation index (NDVI) in 2015, which was downloaded from the Geospatial Data Cloud (https://www.gscloud.cn/search). (b) This map shows the three-dimensional shape of the sampling site, which was obtained from Google Earth. (c) The ice nuclei sampler (The TH-150D medium flow sampler, Wuhan Tianhong Corporation, China).

14. L117: Was there any pretreatment of the PCTE filters?

Response: We did not pretreat the PCTE filters prior to sampling.

15. L117-124: For clarity, maybe specify what each filter sample type was used for, i.e. PCTE for INP analysis, PM2.5 for chemical composition.

Response: Thanks. We have added specific descriptions in the revised manuscript.

16.L120: There were 24 samples taken covering roughly 30% of the entire measurement campaign. The authors may want to comment on the underlying measurement strategy and providing more concrete information under which meteorological conditions samples were taken.

Response: Thanks for the comments. In this study, a total of 24 samples were collected on PCTE filters from August 10 to 24, 2021, which included 2 blank filters. Notably, our observation period coincided with a significant reduction in human activities following the strict lockdown measures enforced after August 10 (refer to response to comment 10). As demonstrated in Figure R1 (and also in Figure S1), the concentration of NOx decreased markedly from 3.0±2.1 ppb during July 24 to August 9 to 0.9±0.3 ppb between August 10 and August 24. This effectively minimizes the influence of human activities on the collection of INPs samples.

17. L120: The chemical analysis was conducted on the samples collected using a PM2.5 inlet. Can the authors estimate the number of particles larger than 2.5 µm which contributed to the INP analysis samples, but would not be covered in the chemical analysis? Has there been any parallel size measurements supporting that claim?

Response: We apologized that we did not collect the INPs at different stages and we had no parallel size measurement to differentiate the particle chemical concentrations between particles larger than 2.5 µm and those smaller than 2.5 µm. This may result in some uncertainties in the investigation of the sources of INPs based on $PM_{2.5}$ chemical composition. These uncertainties have been addressed in the revised manuscript.

18. L130: For consistency, specify the type of weather station.

Response: The Tianchi weather station is an institution under the Changbai Mountain Meteorological Bureau and is affiliated with the National Meteorological Station. We added the information in the revised manuscript: "Meteorological data, such as temperature, humidity, WS, wind direction, pressure, and precipitation, were monitored by the Tianchi weather station, a national meteorological station located approximately 20 m from the sampling site."

19. L153: above -> at

Response: Thanks, we have revised the manuscript accordingly.

20. L158: What was the value of Vair?

Response: V_{air} ranged from 0.035 L - 7.2 L.

21. L159: If the INP concentrations were given in standard liters, the reviewer would advise to indicate this by using e.g., sL-1, or stdL-1 in Equation 3 and corresponding INP data plots.

Response: In the explanation of the N_{INP} calculation formula, we described the computations conducted in standard liters. Following the approach employed by Chen et al. (2018; 2021), we intend to keep this explanation in the main text while excluding it from the INP data plots.

22. L178: Which PBL data product was used? The reviewer could not find a unique record. Furthermore, what is the uncertainty and sensitivity of the PBL data product? Is Changbai mountain centered in a grid box that data was taken from or were different adjacent grid boxes averaged? Given the complex terrain of the mountainous region, how reliable does a 25km x 20km grid box represent the PBL height? Generally, the reviewer is a bit skeptical of the representativeness for the presented application. The authors should elaborate why this data is applicable. In addition, are there any direct meteorological (especially wind) observations along the mountain slope that would support the later claim of vertical transport due to orographic lifting?

Responds: The PBL data was obtained from the fifth-generation ECMWF global atmospheric reanalysis (ERA5 reanalysis). This dataset has been widely used in numberous studies, such as Le et al. (2020), Tornow et al. (2021), and Slattberg et al. (2022). Guo et al. (2021) conducted a comparative analysis of ERA5 reanalysis products against other widely used products, i.e., MERRA-2, JRA-55, and NCEP-2. The results showed that the ERA5 exhibited the smallest bias. Therefore, we have confidence in the reliability of the PBL data sourced from ERA5 for our analysis.

In the input meteorological dataset, specifically the Global Data Analysis System (GDAS) data, Changbai Mountain's terrain height is recorded at 1656 m. In our simulation, we utilize a trajectory ending height of 967 m (above ground level), to achieve a sampling station elevation of 2623 m.

As show in Figure R3a , the 72-hour backward trajectories showed that prevailing air masses predominantly approached the sampling site from the east. However, local winds exhibited a prevailing pattern from the west and south. As elucidated in section 2.1, the Changbai Mountains exhibit a topography characterized by the higher elevations in southeast compared to the northwest. Our observation site is situated in the north of Tianchi Lake. Air masses arriving from the east encounter obstruction by the Changbai Mountains, resulting in a lifting along the southern to western slopes. Figure R3d showed the trajectory heights of the air masses during the daytime. It is evident that as they approached the observation sites, their trajectories inclined upward along the southern or southwestern mountainsides (Figure R3b). This suggests that the air masses underwent a noticeable lifting process prior to reaching the sampling site,

potentially attributed to orographic lifting along the mountain slopes in the south and west directions.

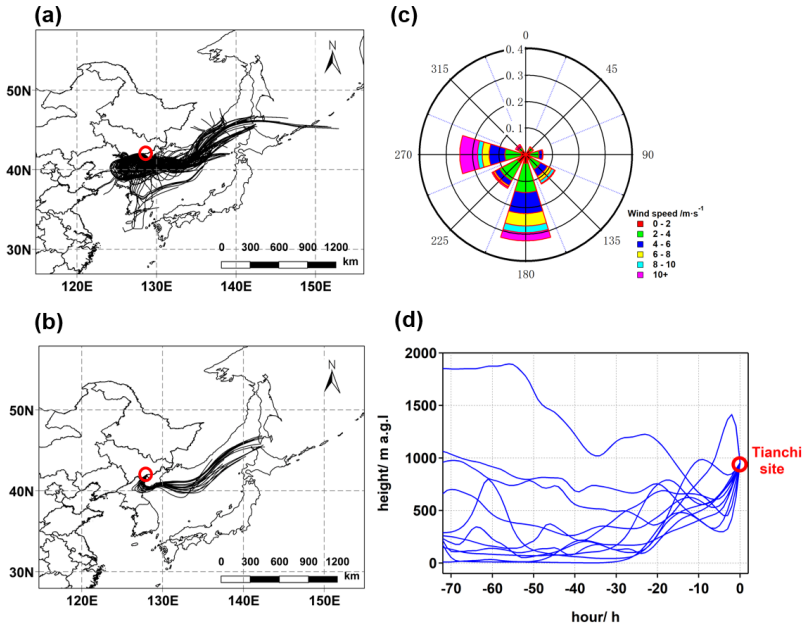

Figure R3. Air mass trajectories over the entire campaign duration (a) and Aug. 13, 2021 (b). Wind rose illustrating wind speed and directions measured in one-minute time resolution at the sampling site (c). and the average daytime air mass trajectory heights (d).

23. L184: The authors may want to briefly describe the principle of CWT.

Responds: We have added the description of CWT in Section 2.5 as follows:
"The CWT assigns the average weighted concentration by trajectories were divided into grids. The calculation was used Equation 5 according to the method of Hsu et al. (2003):

$$C_{ij} = \frac{1}{\sum_{k=1}^{M} \tau_{ijk}} \sum_{k=1}^{M} C_k \tau_{ijk}, \quad (5)$$

where C_{ij} is the average weighted concentration in the ij cell, k is the index of the trajectory, M is the total number of trajectories, C_k is the concentration observed on arrival of trajectory k in the ij cell, and τ_{ijk} is the time spent in the ij cell by trajectory. The weight function W_{ij} was also applied to the CWT analysis to reduce the uncertainty in the cells with small values of n_{ij}:

$$WCWT_{ij} = C_{ij} \times W(n_{ij}), \quad (6)$$"

Results and Discussion

24. L190: "characterize situation of droplet freezing" sounds odd.

Responds: In the revised manuscript, we have revised this sentence to make it more readable: "A metric was applied to evaluate the freezing of droplets, i.e., the freezing temperature at which 50% of the droplets are frozen (T50)."

25. L192: As there are only two MilliQ water backgrounds displayed, rephrase to "were -30°C and -28.5°C".

Response: We conducted measurements on more than two MilliQ water samples, as displayed by the purple lines in Figure R4.

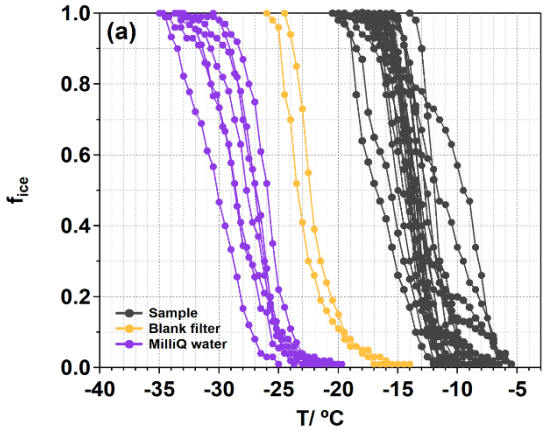

Figure R4. Frozen fractions (f_{ice}) as functions of temperature. The f_{ice} of collected samples measured by GIGINA is shown by the black curves, and presented together with blank filters (orange curves) and MilliQ water (purple curves) as background signals.

26. L193-196: This seems contradicting. If the contaminants could be ignored, one would not need to correct for it.

Response: We agree and therefore revised the statement as follows: "The T_{50} of MilliQ water ranged from −30.0 °C to −26.0 °C, reflecting the low background value of the droplet-freezing apparatus. For the blank filters, T_{50} was averaged to −24.2 ± 2.1 °C, which was slightly higher than that of MilliQ water, but significantly lower than that of the collected samples (for which T_{50} was −17.0 ± 4.1 °C). This result suggests the presence of minimal contaminants stemming from the filter membrane."

27. L195-196: Were averaged concentrations at each temperature step of the two blank filter samples subtracted as correction – please specify. As two samples are not many, the authors may want to comment on the overall obtained repeatability of blank filter measurements obtained which are not presented in this study.

Response: We collected blank filters during both daytime and nighttime, as listed in Table R1. The sampling duration lasted for 11 hours, and we believe that the two blank samples could adequately represents the background values of the filters. During the calculation process, we applied corrections by subtracting the values obtained from the two blank filter samples at each freezing temperature.

28. L199: -26.0°C -> -20°C

Response: Thank you for the comment. In the revised manuscript, we have updated the temperature value from "-26.0°C" to "-29°C." This modification was made because we diluted the samples to obtain the N_{INP} spectra at lower freezing temperature.

29. L200: What it the values of T50? -13°C from above? The authors should repeat this value here, or introduce another variable to avoid the nomenclature confusion of T50 representing the result of one sample (L191) or the average of all samples (L194).

Response: Thank you for the comment. The T_{50} was -17°C based on the full freezing temperature spectra from −29.0 °C to −5.5 °C. We have made the corrections in the revised manuscript.

30. L201: It is not necessarily the diversity of different INPs but could also just relate to different emission strengths.

Response: Thanks for the comment. We have removed the statement in the revision.

31. L202: What would that local source be?

Response: We apologize for the vague wording. In the revision, it has been modified to read as follows: "Some of the N_{INP} curves exhibited bumps in the HTR, which has been also observed at a coastal site (the Cape Verde Atmospheric Observatory, Africa) by Welti et al. (2018) in air samples and in the upper bound of the composite nucleus spectrum of cloud water and precipitation samples by Petters and Wright (2015). Welti et al. (2018) reported that the narrower the IN properties, the steeper slope can be observed in a temperature spectrum".

32. L205-206: This statement cannot be made, as it seems that there have no dilutions of samples been made. This sets the upper limit in detectable NINP = 1/Vair i.e., all droplets frozen.

Response: In the revised manuscript, we extended the freezing temperature below -25°C by diluting the samples. Firstly, we re-measured INP concentrations for the original samples, and found that the concentration of N_{INP}, $N_{INP\text{-}heat}$, and $N_{INP\text{-}H2O2}$ were basically consistent between the latest measurements and previously recorded concentrations (Figure R5). Subsequently, we diluted the suspension liquid by the factors of 30, 60, and 120 times, ensuring that all samples reached a freezing temperature of at least -25°C. Consequently, we have updated the freezing temperature spectra of N_{INP} in the revised manuscript.

Based on the updated data, we are confident in this statement. Here, we have modified the statement in the revised manuscript: "In contrast, in the low-temperature region (LTR, freezing temperature below T_{50}, -17.0 °C ~ -29.0 °C), N_{INP} showed a relatively narrow variation from 0.1 L^{-1} to 78.3 L^{-1}."

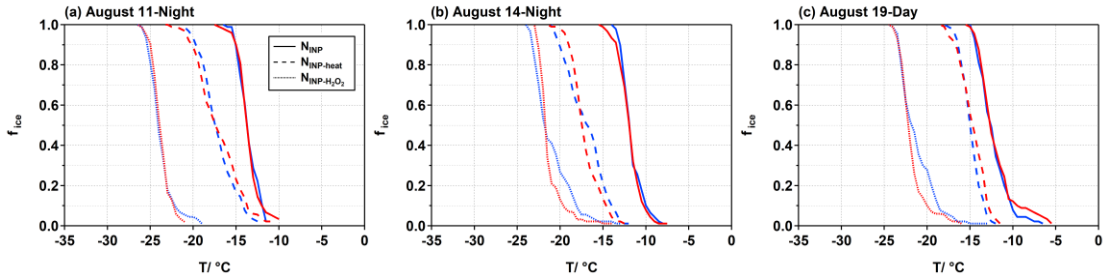

Figure R5. Comparison of frozen fractions (f_{ice}) as functions of temperature between the latest measurements and previously recorded concentrations. The blue and red lines represent the experiment conducted on January 2022 (previous experiment) and September 2023 (latest experiment), respectively.

33. L206: To the reviewer, the temperature dependence results especially from the fact that NINP is cumulative. A direct connection to the complexity of sources cannot be made.

Response: We agree and have removed the statement in the revision.

34. L207: What test was used to check for differences between daytime and nighttime samples?

Response: We conducted an independent t-test, yielding a significance level is 0.61 which is higher than 0.05. Therefore, we concluded that there are no significant differences in N_{INP} between the daytime and nighttime samples.

35. L207-211: It remains questionable if the sampling intervals used in the study (maximally two per day, 20 samples total spread out unknown over a month) allow for the detection of a diurnal cycle. It is conceivable that if, e.g., the minimum in INP concentration occurs at 6:00 and the maximum at 18:00, no difference would be observed on the filters. The described scenario could be likely if the transport is facilitated by convection. In addition, are there any potential local sources located on Changbai mountain, e.g., from the lake, which could cover up a potential diurnal cycle? The authors should elaborate on these aspects.

Response: Our objective is to compare differences in INPs concentration between daytime and nighttime, rather than delve into an extensive analysis of diurnal variations. Factors such as changes in valley breezes, the evolution of the PBL, photochemical reactions, and other variables may exert distinct effects on INPs concentration during these two time periods. Additionally, local sources such as vegetation and the lake could also influence INPs concentration, with biogenic emissions potentially differing between daytime and nighttime.

We agree that our dataset was limited in size, resulting in uncertainties when comparing INPs concentrations between daytime and nighttime. These uncertainties have been addressed in the revised manuscript.

36. L212-226: In the following discussion, references to the data figure could be beneficial. Furthermore, when discussing the obtained results to previous studies, more precision is

needed, what is the difference between "narrowly" (L214) and "much narrower" (L216)? More quantitative expressions are needed. In addition, the present study motivated the need for measurements on high altitude sites. It is not entirely clear, how the sites of Cerro Mirador and Beijing relate to this. Maybe an extra motivation for this comparison would be needed. Studies from high altitude stations like Storm Peak (US), Jungfraujoch (Switzerland), or Altzomoni (Mexico) might be interesting additions, which could also complement Figure 2b, but the reviewer leaves this up to the authors.

Response: In the revised manuscript, we have included temperature range data to provide a more precise explanation of the terms "narrow" and "much narrower."

In the revised Figure 2b, we have excluded the N_{INP} data for Cerro Mirador and Beijing, and added the N_{INP} data for Jungfraujoch and Colorado Rocky Mountains. The corresponding discussions have been added as follows: "In the LTR, our results were comparable to the measurements based on the Storm Peak Laboratory in the northwestern Colorado Rocky Mountains by Hodshire et al. (2022). But in HTR, Conen et al. (2022) measured results in Switzerland higher than our study about 1-3 orders of magnitude, and its aerosolized epiphytic microorganisms contributed most of the INPs to primary ice formation at Jungfraujoch."

37. L213: Precise to Swiss Alps.

Response: Thanks for the comment. We have made the corrections in the revised manuscript.

38. L214: Shouldn't it be high-temperature and low-concentration region and vice versa?

Response: Thanks for the comment. We have revised the statement as follows: "In our observations, the spectra range of N_{INP} were narrowly located in the relatively high-concentration regions at overlapping freezing temperatures compared to the measurements of Wieder et al. (2022)."

39. Section 3.2: The reviewer perceived the usage of the abbreviations bio-INPs, other org-INPs, and inorg-INPs at times a bit odd. If the authors want to keep them, they may want to consider introducing them already in the introduction.

Response: Thanks for the comment. In the introduction, we provided a brief overview of the categories of biological INPs, non-proteinaceous biological INPs, and inorganic INPs to facilitate a better understanding for readers in following sections.

40. L236: Specify type of H2O2

Response: Thanks for the comment. We have added this information in the revised manuscript.

41. L254-256: Was this increase significant and isn't it rather a bias due to the measurement limitations (no dilutions)?

Response: We have updated Figure 3b based on the dilution procedure, and have significantly expanded the dataset at lower temperatures below -25°C. Figure R6 illustrated the revised boxplot depicting fractions of biological INPs, other organic INPs, and inorganic INPs. It can be found that as the temperature decreased from -16.5°C to -21.5°C, the median value of $F_{INP\text{-}bio}$ increased from 0.8 to 0.9. The increase suggests the presence of biogenic INPs with notably high ice-nucleating activity in the LTR.

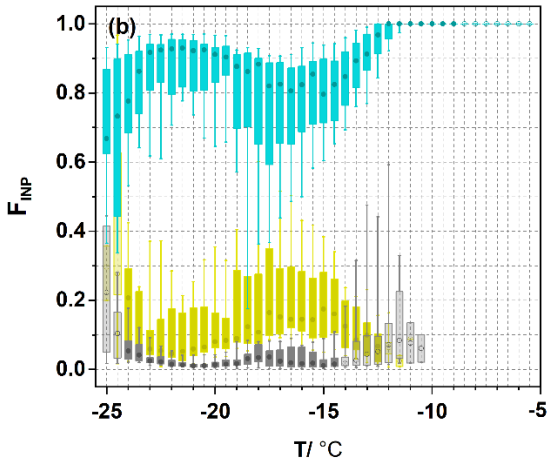

Figure R6. Boxplot of fractions of bio-INPs ($F_{INP\text{-}bio}$, blue boxplot), other org-INPs ($F_{INP\text{-}other\ org}$, yellow boxplot), and inorganic INPs ($F_{INP\text{-}inorg}$, gray boxplot) as functions of temperature. The upper and lower extents of the boxes represent the 75th and 25th percentiles, respectively, while the whiskers indicate the 10th and 90th values. The circle in each boxplot represents the median value. The light-colored boxes indicate that the number of data points is less than half (the sample number is less than 11) of all samples at each temperature.

42. L264: Add the actual number of samples that make up 50% (also in the caption of Fig. 3).

Response: Thanks for the comment. We have added the actual number of samples in the revised figure caption.

43. L269-270: Again, how significant was this increase and is the decrease to low temperatures owed to a measurement bias?

Response: Please see our response to Comment 41.

44. Section 3.3: The data used in this section is unavailable. As the raw data for creating Figure 4 is already quite digested in Figure 4, the authors may want to add a table with the data written out per sample in the appendix. In addition, the found correlations are described as "good" or "weak". As the definitions for these terms may vary, the value and type of used correlation should be named throughout the manuscript.

Response: Thanks for the comment. We have added a table to show the Pearson correlation coefficients in the supplementary materials, as shown in Table R3. In the table caption, we provided a description of the correlations as follows: “When r is below 0.5, the correlation is considered weak; when r exceeds 0.5, the correlation is considered good.” In addition, we have added the r and p values in the revised manuscript.

Table R3. The Pearson correlation coefficients (r) between (a) N_{INP}, (b) $N_{INP\text{-}bio,}$ (c) $N_{INP\text{-}other\ org}$, (d) $N_{INP\text{-}inorg}$ and meteorological parameters, chemical compositions, as functions of temperature. Coefficients reported in bold are statistically significant at $p < 0.05$, while the shades indicate that the number of data points is less than half (the sample number is less than 11) of all samples at each temperature. When r is below 0.5, the correlation is considered weak; when r exceeds 0.5, the correlation is considered good.

	-25	-24	-23	-22	-21	-20	-19	-18	-17	-16	-15	-14	-13	-12	-11	-10	-9	-8	-7
(a)																			
T	**0.63**	**0.61**	**0.63**	**0.64**	**0.60**	**0.51**	0.43	**0.47**	**0.49**	**0.52**	**0.58**	**0.43**	0.16	0.28	0.25	0.19	0.12	0.08	-0.14
RH	**-0.66**	**-0.63**	**-0.69**	**-0.69**	**-0.65**	**-0.6**	-0.44	-0.37	-0.28	-0.26	-0.31	-0.04	0.07	0.03	0.08	0.16	0.09	0.17	0.14
WS	-0.22	-0.28	-0.24	-0.25	-0.2	-0.12	-0.08	-0.2	-0.23	-0.22	-0.23	0.04	0.20	0.36	**0.52**	**0.57**	**0.74**	0.57	0.44
BC	**0.84**	**0.8**	**0.83**	**0.76**	**0.63**	**0.53**	0.34	0.23	0.16	0.1	0.13	-0.11	0.07	-0.06	-0.14	-0.32	-0.28	-0.54	-0.37
$PM_{2.5}$	**0.63**	**0.56**	**0.54**	0.47	0.43	0.42	0.27	0.11	-0.02	-0.04	-0.01	0.04	0.19	0.17	0.07	0	0.17	-0.1	-0.04
NH_4^++NO_3^- +SO_4^{2-}	0.13	0.01	0.09	0.05	0.02	0.05	-0.01	-0.14	-0.18	-0.22	-0.26	-0.43	-0.20	-0.29	-0.18	-0.24	-0.19	-0.57	-0.64
Ca^{2+}	-0.22	-0.27	-0.31	-0.30	-0.24	-0.14	-0.09	-0.13	-0.19	-0.09	-0.14	0.05	-0.05	0.08	**0.64**	0.67	**0.94**	**0.93**	0.71
(b)																			
T	**0.53**	**0.59**	**0.62**	**0.64**	**0.59**	**0.48**	0.37	0.48	**0.54**	**0.5**	**0.57**	**0.44**	0.16	0.27	0.25	0.19	0.12	0.08	-0.14
RH	**-0.58**	**-0.68**	**-0.68**	**-0.69**	**-0.64**	**-0.57**	-0.37	-0.34	-0.28	-0.27	-0.31	-0.05	0.06	0.04	0.08	0.16	0.09	0.17	0.14
WS	-0.17	-0.23	-0.24	-0.24	-0.19	-0.1	-0.1	-0.28	-0.25	-0.21	-0.2	0.11	0.2	0.37	**0.52**	**0.57**	**0.74**	0.57	0.44
Isoprene	0.66	0.45	0.37	0.45	0.5	0.42	0.44	-0.14	-0.13	0.01	0.43	0.44	0.49	0.53	0.63	0.61	0.7	0.66	0.94

Isoprene ×O_3	0.95	0.71	0.7	0.71	0.69	0.51	0.47	-0.09	-0.16	-0.44	0.13	0.03	0.09	0.33	0.65	-	-	-	-
Cl^-	-0.24	-0.32	-0.38	-0.35	-0.31	-0.31	-0.22	-0.15	-0.12	-0.03	-0.05	0.01	-0.15	-0.19	-0.22	-0.31	-0.32	-0.51	-0.43
Ca^{2+}	-0.23	-0.25	-0.32	-0.31	-0.24	-0.15	-0.12	-0.15	-0.18	-0.11	-0.13	0.09	-0.04	0.08	**0.64**	0.67	**0.94**	**0.93**	0.71
(c)																			
T	**0.96**	0.15	**0.51**	0.29	0.28	**0.62**	**0.61**	**0.7**	**0.68**	**0.51**	0.32	0.1	0.16	-0.3	-	-	-	-	-
RH	-	0.02	-0.17	-0.18	-0.23	-0.42	**-0.67**	**-0.44**	-0.33	-0.18	-0.04	0.01	-0.01	0.22	-	-	-	-	-
WS	-0.4	-0.15	-0.12	-0.21	-0.27	-0.33	-0.21	**-0.45**	**-0.46**	**-0.48**	**-0.42**	-0.32	-0.3	-0.17	-	-	-	-	-
Isoprene	-	0.68	0.33	0.24	0.24	0.28	-0.07	0.69	0.7	**0.76**	**0.76**	**0.73**	-0.14	-0.96	-	-	-	-	-
Isoprene ×O_3	-	0.32	-0.6	-0.33	-0.13	-0.13	0.09	0.54	0.58	0.61	0.59	0.64	-0.15	-	-	-	-	-	-
OC	0.85	0.35	0.12	0.32	0.42	0.07	0.2	-0.15	-0.12	-0.16	-0.18	-0.06	0.28	0.43	-	-	-	-	-
EC	0.93	0.36	0.07	0.13	0.25	0	0.18	0.22	0.16	0.27	0.28	0.35	0.31	0.43	-	-	-	-	-
(d)																			
T	0.06	0.26	**0.59**	0.34	0.34	0.36	**0.47**	0.32	0.34	0.1	0.04	-0.28	-0.59	-0.45	-0.56	-	-	-	-
RH	-0.33	-0.32	**-0.7**	**-0.46**	**-0.52**	**-0.53**	**-0.62**	**-0.63**	**-0.64**	-0.5	-0.16	0.38	0.48	0.42	0.65	-	-	-	-
WS	0.28	-0.19	-0.31	-0.16	-0.08	-0.1	-0.13	-0.09	-0.14	0.24	0.08	0.01	0.47	0.49	0.91	-	-	-	-
NH_4^++NO_3^- +SO_4^{2-}	**0.78**	**0.65**	0.46	**0.63**	**0.62**	**0.49**	0.43	0.34	0.36	0.49	0.23	0.41	0.64	0.56	-	-	-	-	-
Cl^-	-0.36	-0.27	-0.37	-0.35	-0.3	-0.43	-0.46	-0.38	-0.32	-0.31	-0.3	-0.32	-0.19	-0.18	-	-	-	-	-
Ca^{2+}	0.34	-0.03	-0.26	-0.31	-0.24	-0.35	-0.32	-0.39	-0.29	0.27	0.39	0.21	-0.18	0.03	-	-	-	-	-

BC	0.28	0.46	**0.85**	**0.74**	**0.74**	**0.78**	**0.8**	**0.83**	**0.74**	0.48	0.24	-0.2	-0.14	-0.16	0.82	-	-	-	-

45. L278-279: Even though the authors selected a mild formulation for their interpretation, this statement should be toned down a little bit more for having only found a good correlation with one element. Furthermore, could there be other sources as well?

Response: We have revised the statement as follows: "Moreover, N_{INP} and Ca^{2+} showed a good positive correlation (r = 0.6-0.9) within the range of -11.0 ℃ to -8.0 ℃, leading us to speculate that soil dust may play an important role in ice nucleation in this temperature range."

In addition to Ca^{2+}, we did not conduct the analysis of other ions originating from soil dust.

46. L281: Kanji et al. 2017 is a summary, maybe use direct study for this reference.

Response: Thanks. We have cited the references, i.e., Hill et al. (2016) and O'sullivan et al., (2014), in the revision.

47. L288-289: Is there reference for this methodology? What was the used threshold in concentration to come to this conclusion?

Response: The dust event is defined as the day when the peak PM_{10} concentration exceeds 150 μg m^{-3} and the $PM_{2.5}/PM_{10}$ ratio falls below 0.4, in accordance with previous studies (Wu et al., 2020; Liu et al., 2006). During our sampling period, $PM_{2.5}$ concentrations ranged from 1.5 μg m^{-3} to 31.6 μg m^{-3}, with an average of 9.3±6.0 μg m^{-3}. Notably, these values remained significantly lower than the established threshold.

48. L306-309: Despite being textbook knowledge, the authors may want to give a reference to read up in these topics. Furthermore, a short description of the essential processes for Changbai mountain could be given in the introduction.

Response: We have cited the references, i.e., Chow et al. (2013) and Wieder et al. (2022) in the revised manuscript.

In the method section, we have added a description of the meteorological conditions as follows: "Changbai Mountain is situated within the westerly wind belt and experiences a typical temperate continental mountain climate influenced by the monsoon, characterized by long cold winters and short temperate summers. The prevailing winds in this region are the westerly and northwesterly winds in the spring, autumn, and winter season and the southeasterly and southwesterly winds in the summer season (Zhao et al., 2015)."

49. L313: Specify "moderate-to-good".

Response: We have added the r values in the revision.

50. L315: "exceptionally high NINP-bio values" add e.g., 'as discussed below' for readability.

Response: Thanks for the comment. We have added "they will be further discussed in the following paragraph" in the revised manuscript.

51. L315-316: Even though being only a suggestion, in the reviewer's opinion this statement cannot be made given too many assumptions and misinterpretation. First, the two high INP cases are excluded and given the argument should coincide with height. Is that an indication for a potential strong but infrequent local source? This might well be pure coincidence, but given the dates being a week apart, was there some periodic event near the measurement site? Second, while the correlation (which type of coefficient?) for some temperature is comparably large, there does not seem to be a significant increase in INP concentration. In addition, if the transport of bio-INP was the underlaying process, one could expect that the correlation should be expressed at a broad range of INP concentrations at a wide range of temperature in the HTR – has this been observed and could the correlation at all temperature been shown, e.g., in a table? Lastly, the PBL height never extends to the mountain top. For transport there is further evidence needed like wind speed and direction along the slope to support this claim. Ultimately, the analysis also bases only on 6-9 datapoints and the uncertainty in the PBL product remains undiscussed.

Response: In the revision, we extended the freezing temperatures below -25°C by diluting the samples, resulting a larger dataset for N_{INP}, especially in the low-temperature region (LTR). Therefore, we re-calculated the correlation that include all samples, without excluding the two high values. The correlation between PBL height and N_{INP} is illustrated in Figure R7. It is evident that the Pearson correlation coefficient between bio-INPs and PBL in the LTR has notably increased compared to the initial calculation. However, in the HTR, there was no correlation between bio-INPs and PBL. For example, Figure R8 (also Figure 5ab in the revision) showed the relationship between bio-INPs and PBL at temperatures at -10.5°C and -21°C. During daytime sampling, bio-INPs and PBL exhibited a good positive correlation at -21°C, but showed no correlation at -10.5°C. However, upon excluding the two high INP cases at-10.5°C, the remaining seven cases exhibited an increasing trend in bio-INPs as PBL height increased ($r=0.77$, $p<0.05$). The two high INP cases may be related to ocean and vegetation emissions when we performed the analysis using the CWT model, and these have been added in the revision.

The backward trajectory in Figure R3d showed that the air mass underwent a noticeable lifting process prior to reaching the sampling site, which could be associated with orographic lifting along the mountain slopes in the south and westward directions. We agree the presence of uncertainties in both the simulation of air mass backward trajectory and the determination of PBL height. These uncertainties have been added in the revised manuscript.

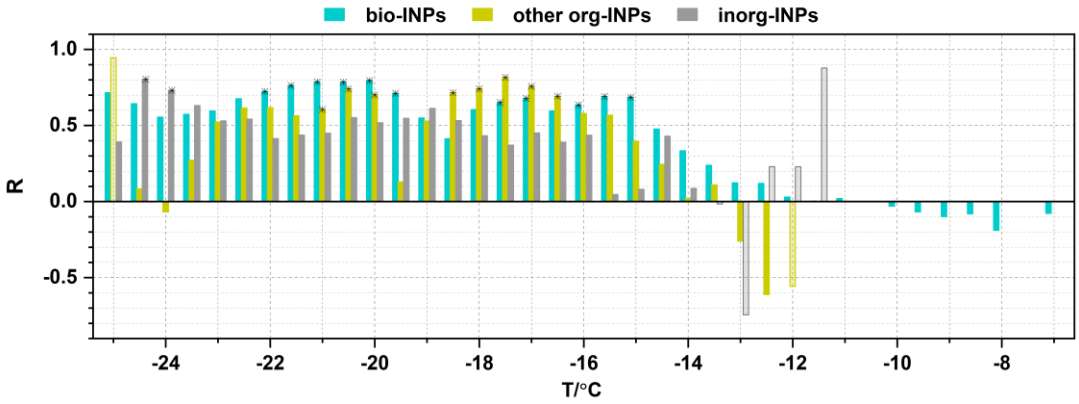

Figure R7. The relationship between PBL height and $N_{INP\text{-}bio}$, $N_{\text{INP-other org}}$ as well as $N_{\text{INP-inorg}}$ during daytime (8:00-17:00, m above ground level) as a function of temperature. The r denote the Pearson correlation coefficients. The asterisk indicates $p < 0.05$. The shades indicate that the data points number were less than half of all samples at each temperature.

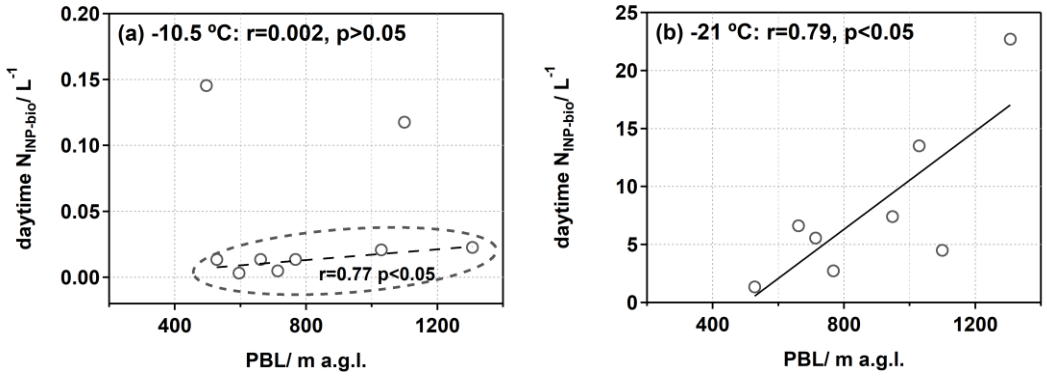

Figure R8. Relationship between $N_{INP\text{-}bio}$ and PBL height during the daytime (8:00–17:00 LT) at freezing temperature of −10.5 °C and −21.0 °C. The r denotes the Pearson correlation coefficients.

52. L316-319: For this claim, data should be presented.

Response: We have provided data in the supplementary materials as Figure S5, as shown in Figure R3d.

53. L328: Add reference for phytoplankton blooms occurrence.

Response: We have added the reference in the revision.

54. L348: Were there still enough datapoints available below

Response: After the dilution experiment, there were enough datapoints below -19.5℃.

55. L357-358: Following Figure S1, it appears to the reviewer, that the correlations for other org-INPs seem similarly or even more consistent throughout the temperature range than for the presented bio-INPs data.

Response: After the dilution experiment, we updated the N_{INP} values and revised Figure S1 (as shown in Figure R7). Generally, bio-INPs and PBL showed good correlations (r=0.4-0.8) in the LTR within the range of -25.0 ℃ to -15.0 ℃, while other org-INPs and PBL showed good correlations (r=0.5-0.8) within the range of -23.0℃ to -20.0 ℃ and -19.0 ℃ to -15.5 ℃. Detail description can be found in the revised manuscript.

Conclusion

56. L364-371: Maybe repeat introduced variables such as FINP-bio, LTR, WS.

Response: We have added an explanation to the abbreviation in the revised manuscript.

57. L377-378: "With larger contributions observed from local and oceanic sources" - was this shown in the results section?

Response: The conclusion has been included in the fifth paragraph of the revised Section 3.4.

58. L379-389: The reviewer is unsure whether diving in to the topic of secondary ice formation in the last paragraph without any prior mention of the topic is within the scope of this publication.

Response: We have removed the discussion of secondary ice formation in the last paragraph in the revision.

59. L384: "confirm" seems to be the wrong word, the statement should be weakened.

Response: We have changed the word to "indicate".

Figures

60. Figure 1: Is it essential to indicate Beijing? If so, it should be named in the caption. To stay consistent between (b) and (a) it could be beneficial to indicate Changbai mountain (check spelling in figure) in red in (a).

Response: We removed the labeling for Beijing and adjusted the text color for the stations in (a) and (b), as shown in Figure R2.

61. Figure 2a: What is the error in T and f?

Response: The error of f_{ice} was 0.002-1.0. To ensure the readability of the information in the figure, we did not display the error bars in Figure 2a.

62. Figure 2b: Specify the data of Wieder et al. 2022 to Weissfluhjoch instead of Alps. The data of Wieder et al. 2022 is not fully visible. Beijing data is hard to read. For better comparability, maybe an average or median of each data set could be added.

Response: We have revised the site names and adjusted the concentration display range on the spectra. The data from Beijing has been removed, and data from the high-altitude stations have been added into Figure 2b, as shown in Figure R9.

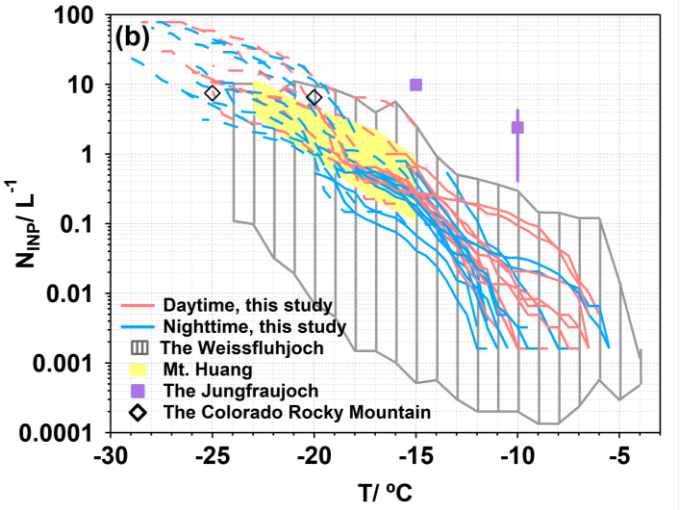

Figure R9. The concentrations of INPs (N_{INP}) as functions of temperature. The dark gray shaded area represents the upper and lower limits of N_{INP} over the Weissfluhjoch (2693 m a.s.l.) (Wieder et al., 2022). The yellow shaded area represents the atmospheric N_{INP} ranges at Mt. Huang (1840 m a.s.l) (Jiang et al., 2015). The purple square represents the median N_{INP} at −15 ℃ and −10 ℃ in the Jungfraujoch (3580 m a.s.l.) (Conen et al., 2022). And the black rhombus represents the median N_{INP} at −25 ℃ and −20 ℃ at the Storm Peak Laboratory in the northwestern Colorado Rocky Mountains (3220 m a.s.l.) (Hodshire et al., 2022).

63. Figure 3a and 3b: Using thin lines instead of dots per spectrum may enhance the readability.

Response: We have made the changes in the revised manuscript.

64. Figure 3a: Error bars extend beyond axis limits. As NINP, NINP-heat, and NINP-H2O2 are only used to calculate NINP-bio, NINP-other org, and NINP-inorg Figure 3a could be moved to appendix to focus on the essential plots 3b and 3c.

Response: We modified the N_{INP} concentration display range on the spectra, and moved the figure to Supplementary Information.

65. Figure 3b: Are all the calculated differences in concentration significant? Could (exemplary) error bars be added?

Response: The presence of error bars can sometimes obscure the information in the figure. Consequently, we have presented the error bars in Figure R10, and added it in the supporting information.

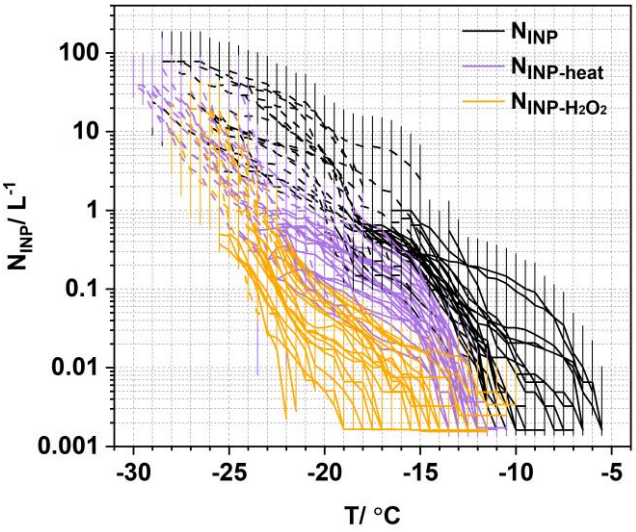

Figure R10. The N_{INP}, $N_{INP\text{-}heat}$, and $N_{INP\text{-}H2O2}$ as function of temperature. The solid line and dotted line show the sample measurement result by immersed in 5 mL MilliQ water and diluted the sample 30-120 times, respectively. The original N_{INP} is marked by black dots, $N_{INP\text{-}heat}$ is marked by purple dots, and $N_{INP\text{-}H2O2}$ is marked by pink dots, with 20% error bars indicating the 95% confidence intervals.

66. Figure 4a: Figure missing.

Response: Thanks, we added this figure in revised manuscript, as shown in Figure R11.

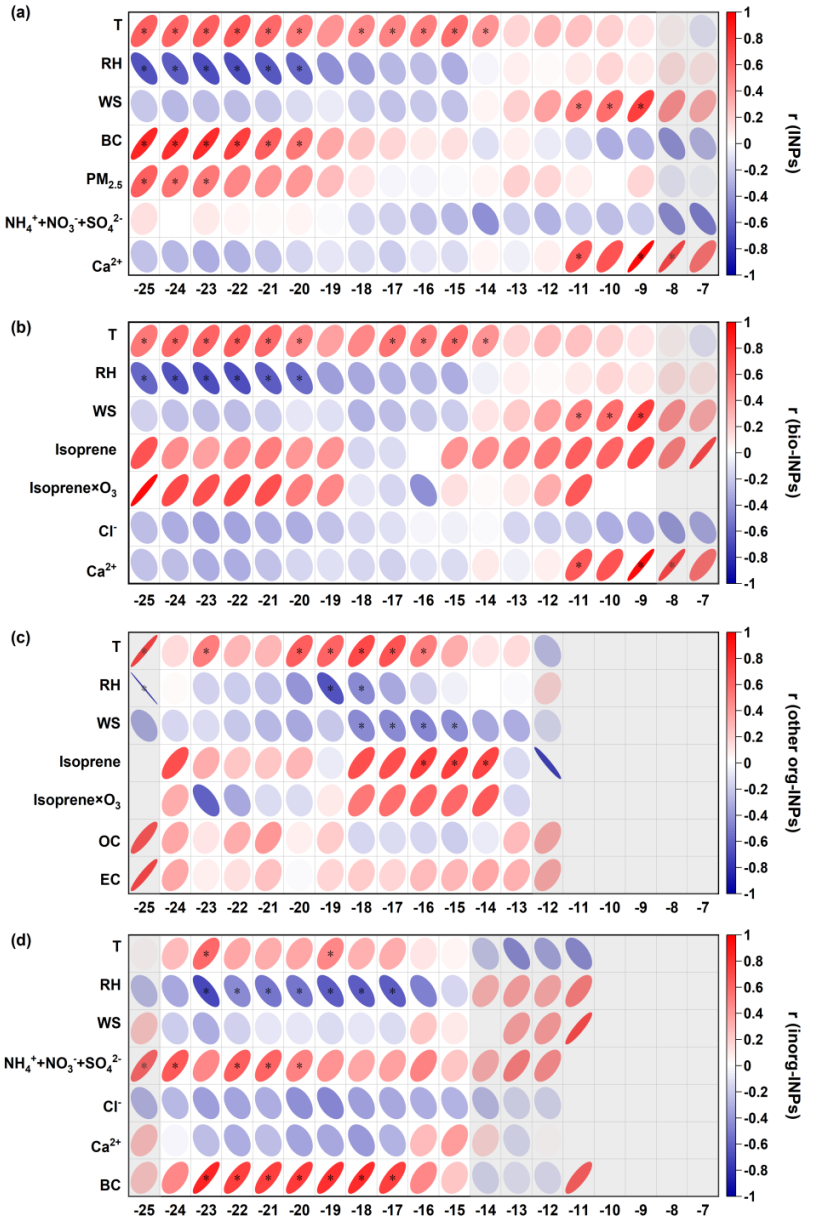

Figure R11. Correlation analysis between (a) N_{INP}, (b) $N_{INP\text{-}bio}$, (c) $N_{INP\text{-}other\ org}$, (d) $N_{INP\text{-}inorg}$, and meteorological parameters, chemical compositions, as functions of temperature. The r denotes the Pearson correlation coefficients. The asterisk indicates $p < 0.05$, while the shades indicate that the number of data points is less than half of all samples at each temperature.

67. Figure 4: As all other figures temperature increases to the right, the x axis of Figure 4 could be flipped for consistency. Which correlation coefficient was used? Specify in caption.

Response: We adjusted the x axis in Figure 4, as illustrated in Figure R11. The Pearson correlation coefficients was calculated, which has been added in the revised manuscript.

68. Figure 5: What is the red star? Is there a specific reason for the y-axis not being logarithmic in contrast to the other plots of INP concentrations?

Response: The red star represents the city of Beijing, which has been removed from the figure. The logarithmic axe is not used because INP concentration is shown at specific freezing temperature, where the range of values is not wide.

Reference:

Chen, J., Wu, Z., Chen, J., Reicher, N., Fang, X., Rudich, Y., and Hu, M.: Size-resolved atmospheric ice-nucleating particles during East Asian dust events, Atmos Chem Phys, 21, 3491-3506, https://doi.org/10.5194/acp-21-3491-2021, 2021.

Chen, J., Wu, Z., Augustin-Bauditz, S., Grawe, S., Hartmann, M., Pei, X., Liu, Z., Ji, D., and Wex, H.: Ice-nucleating particle concentrations unaffected by urban air pollution in Beijing, China, Atmos Chem Phys, 18, 3523-3539, https://doi.org/10.5194/acp-18-3523-2018, 2018.

Chow, F. K., Wekker, S. F. D., and Snyder, B. J.: Mountain Weather Research and Mountain Weather Research and Forecasting: Recent Progress and Current Challenges, Springer Atmospheric Sciences, https://link.springer.com/book/10.1007/ 978-94-007-4098-3 (last access: 21 February 2022), 2013.

Conen, F., Einbock, A., Mignani, C., and Hüglin, C.: Measurement report: Ice-nucleating particles active ≥ -15 °C in free tropospheric air over western Europe, Atmos. Chem. Phys., 22, 3433-3444, 10.5194/acp-22-3433-2022, 2022.

Conen, F., Yakutin, M. V., Yttri, K. E., and Hüglin, C.: Ice Nucleating Particle Concentrations Increase When Leaves Fall in Autumn, Atmosphere-Basel, 8, 202, https://doi.org/10.3390/atmos8100202, 2017.

DeMott, P. J., Prenni, A. J., Liu, X., Kreidenweis, S. M., Petters, M. D., Twohy, C. H., Richardson, M. S., Eidhammer, T., and Rogers, D. C.: Predicting global atmospheric ice nuclei distributions and their impacts on climate, P Natl Acad Sci USA, 107, 11217-11222, https://doi.org/10.1073/pnas.0910818107, 2010.

Guo, J., Zhang, J., Yang, K., Liao, H., Zhang, S., Huang, K., Lv, Y., Shao, J., Yu, T., Tong, B., Li, J., Su, T., Yim, S. H. L., Stoffelen, A., Zhai, P., and Xu, X.: Investigation of near-global daytime boundary layer height using high-resolution radiosondes: first results and comparison with ERA5, MERRA-2, JRA-55, and NCEP-2 reanalyses, Atmos. Chem. Phys., 21, 17079-17097, https://doi.org/10.5194/acp-21-17079-2021, 2021.

Hill, T. C. J., DeMott, P. J., Tobo, Y., Fröhlich-Nowoisky, J., Moffett, B. F., Franc, G. D., and Kreidenweis, S. M.: Sources of organic ice nucleating particles in soils, Atmos. Chem. Phys., 16, https://doi.org/7195-7211, 10.5194/acp-16-7195-2016, 2016.

Hodshire, A. L., Levin, E. J. T., Hallar, A. G., Rapp, C. N., Gilchrist, D. R., McCubbin, I., and McMeeking, G. R.: Technical Note: A High-Resolution Autonomous Record of Ice Nuclei Concentrations for Fall and Winter at Storm Peak Laboratory, Atmos. Chem. Phys. Discuss., 2022, 1-15, https://doi.org/10.5194/acp-2022-29, 2022.

Hsu, Y.-K., Holsen, T. M., and Hopke, P. K.: Comparison of hybrid receptor models to locate PCB sources in Chicago, Atmospheric Environment, 37, 545-562, https://doi.org/10.1016/S1352-2310(02)00886-5, 2003.

Jiang, H., Yin, Y., Su, H., Shan, Y. P., and Gao, R. J.: The characteristics of atmospheric ice nuclei measured at the top of Huangshan (the Yellow Mountains) in Southeast China using a newly built static vacuum water vapor diffusion chamber, Atmos Res, 153, 200-208, https://doi.org/10.1016/j.atmosres.2014.08.015, 2015.

Kanji, Z. A., Ladino, L. A., Wex, H., Boose, Y., Burkert-Kohn, M., Cziczo, D. J., and Krämer, M.: Overview of Ice Nucleating Particles, Meteorological Monographs, 58, 1.1-1.33, https://doi.org/10.1175/amsmonographs-d-16-0006.1, 2017.

Lau, K. M. and Wu, H. T.: Warm rain processes over tropical oceans and climate implications, Geophys Res Lett, 30, 5, https://doi.org/10.1029/2003gl018567, 2003.

Le, T. H., Wang, Y., Liu, L., Yang, J. N., Yung, Y. L., Li, G. H., and Seinfeld, J. H.: Unexpected air pollution with marked emission reductions during the COVID-19 outbreak in China, Science, 369, 702-711, https://doi.org/10.1126/science.abb7431, 2020.

Mulmenstadt, J., Sourdeval, O., Delanoe, J., and Quaas, J.: Frequency of occurrence of rain from liquid-, mixed-, and ice-phase clouds derived from A-Train satellite retrievals, Geophys Res Lett, 42, 6502-6509, https://doi.org/10.1002/2015gl064604, 2015.

O'Sullivan, D., Murray, B. J., Malkin, T. L., Whale, T. F., Umo, N. S., Atkinson, J. D., Price, H. C., Baustian, K. J., Browse, J., and Webb, M. E.: Ice nucleation by fertile soil dusts: relative importance of mineral and biogenic components, Atmos. Chem. Phys., 14, 1853-1867, https://doi.org/10.5194/acp-14-1853-2014, 2014.

Petters, M. D. and Wright, T. P.: Revisiting ice nucleation from precipitation samples, Geophys Res Lett, 42, 8758-8766, https://doi.org/10.1002/2015GL065733, 2015.

Slattberg, N., Lai, H. W., Chen, X. L., Ma, Y. M., and Chen, D. L.: Spatial and temporal patterns of planetary boundary layer height during 1979-2018 over the Tibetan Plateau using ERA5, International Journal of Climatology, 42, 3360-3377, https://doi.org/10.1002/joc.7420, 2022.

Tornow, F., Ackerman, A. S., and Fridlind, A. M.: Preconditioning of overcast-to-broken cloud transitions by riming in marine cold air outbreaks, Atmos Chem Phys, 21, 12049-12067, https://doi.org/10.5194/acp-21-12049-2021, 2021.

Wang, Z. W., Gallet, J. C., Pedersen, C. A., Zhang, X. S., Ström, J., and Ci, Z. J.: Elemental carbon in snow at Changbai Mountain, northeastern China: concentrations, scavenging ratios, and dry deposition velocities, Atmos. Chem. Phys., 14, 629-640, https://doi.org/10.5194/acp-14-629-2014, 2014.

Welti, A., Müller, K., Fleming, Z. L., and Stratmann, F.: Concentration and variability of ice nuclei in the subtropical maritime boundary layer, Atmos. Chem. Phys., 18, 5307-5320, https://doi.org/10.5194/acp-18-5307-2018, 2018.

Wieder, J., Mignani, C., Schär, M., Roth, L., Sprenger, M., Henneberger, J., Lohmann, U., Brunner, C., and Kanji, Z. A.: Unveiling atmospheric transport and mixing mechanisms of ice-nucleating particles over the Alps, Atmos Chem Phys, 22, 3111-3130, https://doi.org/10.5194/acp-22-3111-2022, 2022.

Wu, C., Zhang, S., Wang, G. H., Lv, S. J., Li, D. P., Liu, L., Li, J. J., Liu, S. J., Du, W., Meng, J. J., Qiao, L. P., Zhou, M., Huang, C., and Wang, H. L.: Efficient heterogeneous formation of ammonium nitrate on the saline mineral particle surface in the atmosphere of East Asia during dust storm periods, Environ Sci Technol, 54, 15622-15630, https://doi.org/10.1021/acs.est.0c04544, 2020.

Zhao, X., Kim, S.-K., Zhu, W., Kannan, N., and Li, D.: Long-range atmospheric transport and the distribution of polycyclic aromatic hydrocarbons in Changbai Mountain, Chemosphere, 119, 289-294, https://doi.org/10.1016/j.chemosphere.2014.06.005, 2015.

Anonymous Referee #3

General comments

The manuscript by Sun et al. reports INP measurements at Changbai Summit in the summer of 2021. Using results from heat and H2O2 treatments, the authors distinguish between biological INPs, other organic INPs, and inorganic INPs and conclude that the majority of INPs in the temperature range studied were of biological origin. It is an interesting study that provides new information about biological INPs. They discuss correlations of biological INPs with meteorological data as well as with some chemical tracers, suggesting that biological INPs may originate from soil dust. In addition, possible sources and transport mechanisms of INPs are discussed based on knowledge of the height of the planetary boundary layer and the concentration-weighted backward trajectories of air masses. The authors have made an effort to explain their data, but given the small number of samples (22 in total, half of which were collected during the day and the other at night) and the lack of sample dilutions to extend the freezing spectra to lower temperatures, some sections require substantial revision in my opinion. I have major and minor comments that I hope will be helpful to the authors and can be addressed during the review process.

Response: We are grateful to the reviewer for the valuable comments. During the observation period, a total of 22 samples were collected. Recognizing the potential for uncertainties due to the limited data size, we have addressed this concern in the revised manuscript. Furthermore, we have conducted dilution of the untreated and heat-treated samples and extended the freezing temperature below -25°C. We updated the N_{INP} spectra and corresponding analyses in the revised manuscript. We have endeavored to respond to these valuable comments and revise our manuscript accordingly. Detailed point-to-point responses are shown below.

Specific comments

Abstract

1. Line 12: "modifying" is maybe not the right word here.

Response: We change the "modifying" to "modulating" in the revised manuscript.

2. Lines 22-24: While this insight into atmospheric dynamics is welcome, I would note that this positive correlation between biological INPs with planetary boundary layer height is based on 7 data points only. 2 outliers were excluded and 2 missing data points were not mentioned. It is not stated which correlation analysis was done, something that persists throughout the study. Furthermore, it is unclear for the reviewer how these two cases of high concentrations of biological INPs differ from the other samples in terms of long-range transport. These results

need thorough review, discussions about them need to be clarified, and the relevant conclusions probably need to be revised.

Response: In the revised manuscript, we performed dilutions of the samples by the factors of 30, 60, and 120 times, ensuring that all samples reached a freezing temperature of at least -25°C. We re-calculated the Pearson correlation coefficients that include all samples, including the two high values. The correlations between PBL height and N_{INP} are presented in Figure R1.

The two missing data corresponded to the blank filters, and we have provided clarification regarding this in the revised manuscript. Nevertheless, the data points ranged from 6 to 11 when calculating the Pearson correlation coefficients, resulting in uncertainties. The uncertainties have been addressed in the revised manuscript. Since the revised correlation analysis included the two cases with high concentrations of biological INPs, we have refrained from adding extensive discussions on these two cases.

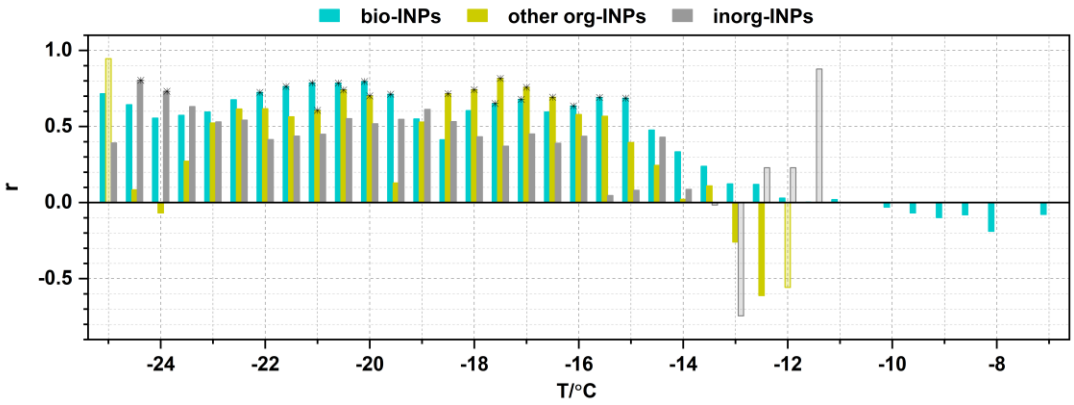

Figure R1. The relationship between PBL height and $N_{INP\text{-}bio}$, $N_{INP\text{-}other\ org}$ as well as $N_{INP\text{-}inorg}$ during daytime (8:00-17:00, m above ground level) as a function of temperature. The r denotes the Pearson correlation coefficients. The asterisk indicates $p < 0.05$. The shades indicate that the data points number were less than half of all samples at each temperature.

Introduction

3. The reviewer thinks that some parts of the introduction should be worded more precisely.

Response: Thanks for the comment. We rewrote some parts of the introduction to make it more precisely.

4. Line 40 and line 52: Please use "etc" carefully. Try to list fully instead.

Response: Thanks for the comment. We have made revisions in the revised manuscript.

5. Line 40: There are also efficient proteinaceous cell-free INPs (Pummer et al., 2015) that are not embedded in cell membranes. Please, reformulate the sentence.

Response: In revision, we have revised the statement as follows: "Biological aerosols such as microbial and proteinaceous origin, containing proteins in cell-free macromolecules or intact cell membranes, demonstrate significant efficiency as INPs at temperatures above −15 ℃ (Phelps et al., 1986; Petters and Wright, 2015; Murray et al., 2012; Kunert et al., 2019; Huang et al., 2021)"

6. Line 45: I am unsure what is meant by "and [in] agricultural soils". Do you mean a site, where presumably many INPs come from particles from agricultural soils? Please reformulate.

Response: The term "and [in] agricultural soils" means the presence of INPs from regions with agricultural soils. In the revised manuscript, we have removed this statement to make the introduction more concise.

7. Line 68: The tree sites that are referred to are not all located in the Swiss Alps, but are located across Switzerland.

Response: Thanks for the comment. We have revised this statement as follows: "For example, in the Switzerland, simultaneous measurements taken at different-altitude stations revealed a reduction of approximately 50% per kilometer in the abundance of INPs in the vertical gradient (ranging from 489 m above sea level (a.s.l.) to 3580 m a.s.l. in the Swiss Alps) in the warm season (Conen et al., 2017)."

8. Lines 70-71: Instead of "one order of magnitude", you could keep the same units as in the previous sentence. Maybe summarize in percent per kilometer.

Response: In the revised manuscript, we replaced "one order of magnitude" with "exceed 60%".

9. Line 72: The "atmosphere" can only be in singular.

Response: Thanks for the comment. We have made the corrections in the revised manuscript.

10. Lines 72-75: Please mention that Schrod et al. 2017 findings were obtained during specific events, i.e., a series of elevated Saharan dust plumes.

Response: In the revision, we have revised as: "In contrast, Schrod et al. (2017) reported an increase in INPs abundance of approximately 10 times over the eastern Mediterranean (2500 m a.s.l.) relative to ground level using unmanned aircraft systems, with this difference attributed

to the long-distance transport of a series of elevated Saharan dust plumes at the height of a few kilometers."

11. Lines 75-77: The citation Conen et al. 2022 is missing at the end of the sentence. I would suggest adding here the following specification: "under free-tropospheric conditions". Study could have been mentioned in L. 44-45 instead/as well.

Response: Thanks for the comment. We have cited the reference in the revised manuscript.

12. Line 87: "INPs measurements" --> "INP measurements"

Response: Thanks for the comment. We have made the corrections in the revised manuscript.

Methods

The reviewer found that the methods are well described, and that it was helpful that the authors provided the raw data for the reviewers.

13. Line 119: Please specify that your times are meant in local time or mention the correct time zone.

Response: We used the local time and have added the description in the revised manuscript.

14. Line 120: A total of 24 samples were collected for INP analysis. The results of only 22 samples were reported in the provided data file. Could the authors please explain why the results of two samples are missing? Could it maybe be that 22 samples and 2 background filters were collected?

Response: Yes, the 24 samples include two background filters. In the revised manuscript, we have modified the statement to: "A total of 24 PCTE filters were collected, including 22 aerosol samples and 2 blank filters." In addition, detailed sampling information has been added in Table S1 in the Supporting Information, as presented in Table R1.

Table R1. Detail information including sampling date, duration and total sampling volume in this study.

Sample Date	Start time	End time	Duration/ min	Total Volume/ L
2021.8.10-Night	2021/8/10 18:00	2021/8/11 5:30	294	34500
2021.8.11-Day	2021/8/11 10:30	2021/8/11 17:30	168	21000
2021.8.11-Night	2021/8/11 18:00 2021/8/11 20:32	2021/8/11 20:26 2021/8/12 3:32	242	28300
2021.8.12-Day	2021/8/12 6:00	2021/8/12 17:30	294	34500
2021.8.12-Night	2021/8/12 18:00	2021/8/13 5:30	294	34500
2021.8.13-Day	2021/8/13 6:00	2021/8/13 17:30	294	34500
2021.8.13-Night	2021/8/13 18:00	2021/8/14 5:30	294	34500
2021.8.14-Day	2021/8/14 6:00	2021/8/14 17:30	294	34500
2021.8.14-Night	2021/8/14 18:00	2021/8/15 5:30	294	34500
2021.8.15-Day	2021/8/15 6:00	2021/8/15 18:00	288	36000
2021.8.15-Night	2021/8/15 18:30	2021/8/16 5:30	264	33000
2021.8.16-Day	2021/8/16 6:00	2021/8/16 17:30	294	34500
2021.8.16-Night	2021/8/16 18:00	2021/8/17 5:30	294	34500
2021.8.17-Day	2021/8/17 6:00	2021/8/17 17:30	294	34500
2021.8.17-Night	2021/8/17 18:00	2021/8/18 5:30	294	34500
2021.8.18-Day	2021/8/18 10:00	2021/8/18 17:30	198	22500
2021.8.18-Night	2021/8/18 18:00	2021/8/19 5:30	294	34500
2021.8.19-Day	2021/8/19 6:00	2021/8/19 17:30	294	34500
2021.8.19-Night	2021/8/19 18:00	2021/8/20 5:30	294	34500
2021.8.20-Day	2021/8/20 6:00	2021/8/20 17:30	294	34500
2021.8.20-Night	2021/8/20 18:00	2021/8/21 5:30	294	34500
2021.8.21-Day	2021/8/21 6:00	2021/8/21 17:30	294	34500
Blank-Night	2021/8/23 17:29	2021/8/24 5:36	295	-
Blank-Day	2021/8/24 7:30	2021/8/24 18:50	284	-

15. Line 130: It would be interesting to know how far the weather station is from the measurement site.

Response: We added the distance description in the revised manuscript: "Meteorological data, such as temperature, humidity, WS, wind direction, pressure, and precipitation, were monitored by the Tianchi weather station, a national meteorological station located approximately 20 m from the sampling site."

16. Lines 178-186: Please be more precise how you generated the air mass backwards trajectories and add information about starting time as well as number of trajectories per sample.

Response: We calculated 72-hour air mass backward trajectories at the sampling sites on an hourly basis during our sampling days. A total of 264 trajectories were generated. These have been added in the revision.

17. Line 188: Which data product from the Climate Data Store did you use for the PBL data?

Response: The PBL data was obtained from the fifth-generation ECMWF global atmospheric reanalysis (ERA5 reanalysis). We have added this information in the revised manuscript.

Results and Discussion

The reviewer found that some parts of the results and discussion need thorough revision and much clearer statements.

18. Line 208 and lines 210-211: Wieder et al. (2022) contains INP concentrations from a mountain site called Weissfluhjoch (2693 m a.s.l.) and a valley site called Wolfgangpass (1631 m a.s.l.). The two sites in the Swiss Alps are only 4 km apart and are not necessarily representative of the entire Swiss Alps. Please be more specific: a) Swiss Alps and not any Alps, b) add the name of the site(s) you mean.

Response: Thanks. We have revised "Alps" to "Weissfluhjoch in the Swiss Alps" in the revision.

19. Lines 208-211: Please provide the time spans for collection and averaging for these other studies. For example, Wieder et al. (2022) collected samples over short time spans (i.e., 20 minutes) and averaged them into 2-hour bins. They found a peak at 19 h UTC (i.e., 21 h CET), which is defined as nighttime based on the definition used in this manuscript, if I am not mistaken. A possible diurnal cycle at Changbai Mountain may have been averaged out due to the long sampling time of 11 hours. Please mention specifically for Changbai Mountain only

the comparison of daytime and nighttime, since only two samples are taken per day. In my opinion, a conclusion over the entire diurnal cycle cannot be made here.

Response: Thanks for the comment. The time spans have been added in the revision. In this study, our objective is to compare differences in INPs concentration between daytime and nighttime, rather than delve into an extensive analysis of diurnal variations. In the revision, we have added the statement as follow: "Additionally, the limited data size and low sampling frequency may also result in a lack of diurnal variation in this study."

20. Line 213: What is meant by "the temperature spectra showed a wider range"?

Response: Thanks for the comment. We have removed the statement in the revision.

21. Line 217: What is meant by "the NINP value was much larger at Mt. Huang than our results"? Can't the difference between both sites be explained by the fact that your results cover a warmer temperature range than the results from Mt. Huang? Please mention the freezing temperatures while comparing INP concentrations.

Response: Based on our updated N_{INP} values after the dilution procedure, we have revised the statement as follows: "Jiang et al. (2015) reported that the INP concentrations at the top of Mt. Huang spanned from 0.1 L^{-1} to 11.9 L^{-1} over a temperature range from -15.0 °C to -23.0 °C, which overlapped with our results."

22. Line 256: Shouldn't it be "bio-INP" instead of "INP"?

Response: Thanks. We have made the corrections in the revised manuscript.

23. Line 254-256: A mean increase in FINP-bio from 0.8 to 0.9 with decreasing temperatures between -16.5 °C and -20 °C doesn't make much sense and could be due to the way the data were processed here. It looks like some untreated and heat-treated samples already reached the upper detection limit at about -15 °C or -16 °C. In order to draw conclusions about the proportion of bio-INPs, other org-INPs, and inorganic INPs below -15 °C, I believe dilutions of the untreated and heat-treated samples would have been required. The number of data points of FINP-bio from maybe around -18 °C and lower is likely too low to draw any conclusions below that temperature threshold.

Response: In the revised manuscript, we diluted the untreated and heat-treated samples by the factors of 30, 60, and 120 times, and extended the freezing temperature below -25°C (details can be found in the response to comment 2). Based on the updated N_{INP} data, we have made revisions to the boxplot, as shown in Figure R2. It can be found that as the temperature decreased from -16.5°C to -21.5°C, the median value of $F_{INP\text{-}bio}$ increased from 0.8 to 0.9. The

increase suggests the presence of biogenic INPs with notably high ice-nucleating activity in the LTR.

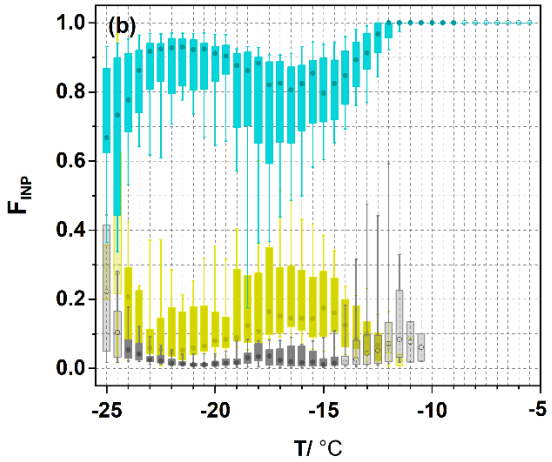

Figure R2. Boxplot of fractions of bio-INPs ($F_{INP\text{-}bio}$, blue boxplot), other org-INPs ($F_{INP\text{-}other\ org}$, yellow boxplot), and inorganic INPs ($F_{INP\text{-}inorg}$, gray boxplot) as functions of temperature. The upper and lower extents of the boxes represent the 75th and 25th percentiles, respectively, while the whiskers indicate the 10th and 90th values. The circle in each boxplot represents the median value. The light-colored boxes indicate that the number of data points is less than half (the sample number is less than 11) of all samples at each temperature.

24. Lines 277-281: What about biological INPs originating from plants and oceans? Please discuss.

Response: Since N_{INP} was positively correlated with WS and Ca^{2+}, we emphasis the discussion of soil source. In Section 3.4, we discuss the marine and plant sources.

25. Lines 279-281: Maybe instead of citing the review, authors could cite the original studies e.g. Hill et al. 2016 or others.

Response: Thanks. We have cited the references, Hill et al. 2016 and O'sullivan et al., 2014, in the revision.

26. Line 301: Maybe instead of citing the review, authors could cite the original studies.

Response: Thanks. We cited the reference, i.e., Cozic et al. (2008) and Levin et al. (2016), in the revision.

27. Lines 315-321: Could the authors elaborate how the inclusion of these points would change the results and conclusion?

Response: We have update the N_{INP} data based on the diluted process, and the relationship between $N_{INP\text{-}bio}$ and PBL have revised as shown in Figure R1. In the HTR, there was no correlation between bio-INPs and PBL. However, upon excluding the two high INP cases at-10.5°C, the remaining seven cases exhibited an increasing trend in bio-INPs as PBL height increased ($r=0.77$, $p<0.05$), as shown in Figure R3a. The two high INP cases may be related to ocean and vegetation emission sources when we utilizing the CWT model to analyze. These have been added in the revision.

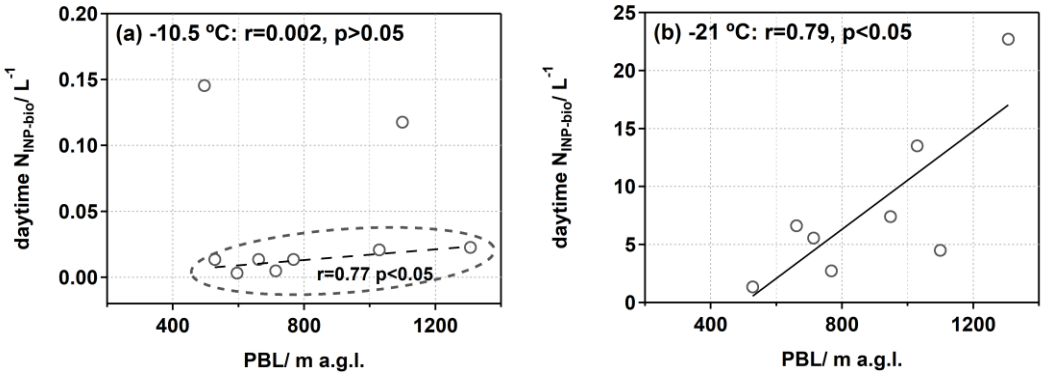

Figure R3. Relationship between $N_{INP\text{-}bio}$ and PBL height during the daytime (8:00–17:00 LT) at freezing temperature of −10.5 ℃ and −21.0 ℃. The r denotes the Pearson correlation coefficients.

28. Line 320: Please indicate here that the "freezing" temperature is meant.

Response: Thanks. As shown in Figure R1, the relationship between PBL and $N_{INP\text{-}bio}$ is greatly improved based on the updated N_{INP} data. Thence, we remove this statement in the revised manuscript.

29. Lines 323-325: How does the CWT analysis on August 18 and 25 differ from the other days?

Response: We have conducted a correlation analysis on the entire dataset and did not delve further into the two high values.

Conclusion

The reviewer believes that some rewording needs to be done, especially in the last paragraph.

30. Lines 365-368: A decreasing trend in FINP-bio with decreasing temperature suggests that other organic or inorganic INPs become more important with decreasing temperatures. It does not suggest that the ice nucleation activity of bio-INPs decreases. In addition, due to the lack of data points in the low temperature regime, no conclusions can be drawn regarding FINP-bio for that temperature range, in my opinion. Dilutions would have been required, as mentioned above.

Response: We agree and modify the statement to "The decreasing trend of $F_{INP\text{-}bio}$ suggested that the importance of bio-INPs decreases with temperature." We have added data in the low freezing temperature range, confirming the conclusions regarding $F_{bio\text{-}INPs}$. Please see our response to comment 23.

31. Line 379: Did you mean to write that the INP number concentration is lower than the ice crystal number concentration, especially in the warm temperature range?

Response: Considering the discussion of secondary ice formation in the last paragraph was not closely aligned with the context of this paper, we have removed it in the revision.

32. Line 381: Is there a word missing between "…is second only to…"?

Response: Considering the discussion of secondary ice formation in the last paragraph was not closely aligned with the context of this paper, we have removed it in the revision.

33. Line 383: Please delete "through various collisions with pre-existing ice". There are several multiplication processes, and they involve many more processes than only ice-ice collision. More information can be found for example in Korolev and Leisner, 2020.

Response: Considering the discussion of secondary ice formation in the last paragraph was not closely aligned with the context of this paper, we have removed it in the revision.

34. Line 385: Bio-INPs do not impact secondary ice formation directly, please reformulate.

Response: Considering the discussion of secondary ice formation in the last paragraph was not closely aligned with the context of this paper, we have removed it in the revision.

Figures

Fig.2(b)

35. Please indicate in the figure and legend the name of the mountain in the Swiss Alps from which the data originate similar to what you did with the Mt. Huang dataset.

Response: We have replaced the name to "Weissfluhjoch".

36. Should the y-axis perhaps be extended to lower values to see the lower limit of the error bar?

Response: We have modified the y-axis to display all the data. But to ensure that the information in the figure can be readily grasped, we did not display the error bar in Figure 2b. The error bar of whole samples was shown in Figure S3, as illustrated in Figure R4.

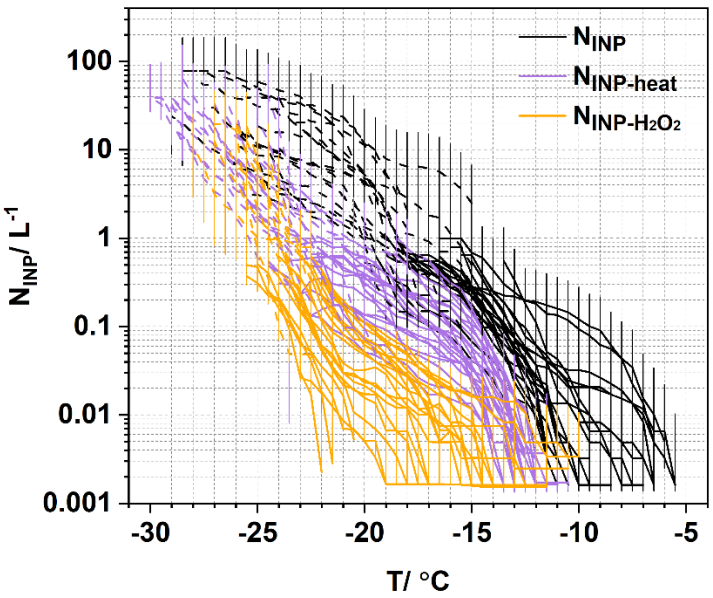

Figure R4. The N_{INP}, $N_{INP\text{-}heat}$, and $N_{INP\text{-}H2O2}$ as function of temperature. The solid line and dotted line show the sample measurement result by immersed in 5 mL MilliQ water and diluted the sample 30-120 times, respectively. The original N_{INP} is marked by black dots, $N_{INP\text{-}heat}$ is marked by purple dots, and $N_{INP\text{-}H2O2}$ is marked by pink dots, with 20% error bars indicating the 95% confidence intervals.

Fig. 3(a)

37. Why are the error bars for NINP-H2O2 below -15 °C extending to values outside the graph?

Response: We adjusted the y-axis range to display all error bars.

38. Please use the same axes in Fig. 3a than in Fig. 3b and Fig. 2b.

Response: We have revised the figures accordingly.

Fig.3(c)

39. I appreciate that there is an indication of the number of data points included in the analysis. Since the upper detection limit of about 2 INPs per liter is reached around -15 °C for NINP-bio, dilutions would have been necessary to extend the plot from -15 to -20 °C as mentioned above.

Response: In the revised manuscript, we extended the freezing temperature below -25℃ by diluting the samples.

40. How can the median fraction of inorganic INPs above -12 °C be more than 0.0 if the median fraction of bio-INPs is 1.0?

Response: We first calculated the daily proportions and then average the proportions across all samples.

Fig.4

41. What kind of correlation analysis did you do? Please specify.

Response: We calculated the Pearson correlation coefficients, which has been added in the revised manuscript.

Fig.5(a-c)

42. What does "r" stand for? Please also describe what the red lines and the purple circles represent.

Response: The r denotes the Pearson correlation coefficients. We have described the manuscript accordingly. The purple circles in original figure represented the exclusion of two high-value data points, and the red line indicated their correlation. However, as mentioned previously, we have updated the data and no longer exclude high values. Instead, we have performed a correlation analysis on the entire dataset. Therefore, revisions have been made, as illustrated in Figure R3.

43. Is the x-axis showing the mean PBL height?

Response: Yes, the x-axis showed the mean PBL height. We have revised the figure caption to "average PBL height during the daytime".

44. Maybe add "freezing" between "three" and "temperatures".

Response: We have revised the manuscript accordingly.

Fig.5 (d-f)

45. Trajectories of which samples were included in the CWT analysis? Are the trajectories of all the samples included or only those of the daytime samples? Were the trajectories of the two outliers excluded or included here? Please be more specific.

Response: All samples were included in the CWT analysis. we have revised the figure caption to "The concentration-weighted trajectory (CWT) analysis for the distribution of $N_{INP\text{-}bio}$ at −10.5 ℃ and −21.0 ℃ during the measurement."

46. Also describe in the legend what the star and triangle represent.

Response: The star represents the capital city of Beijing and has been removed in Figure 5 of the revised manuscript. The triangle represents the measurement site in our study, which we have added accordingly to the manuscript.

Fig. S1

47. Please describe in the legend precisely what is shown and what is meant by "R". Is the large "R" here similar to the small "r" in Fig. 5?

Response: The "R" here was same as the "r" in Figure 5. We used "r" consistently throughout the revised manuscript.

Fig. S2

48. Authors could add the star and the triangle in these maps, similar to Fig. 5 (d-f).

Response: The star represents the capital city of Beijing and has been removed in Figure 5 of the revised manuscript. The triangle represents the measurement site in our study, which we have added accordingly to the manuscript.

Reference:

Conen, F., Yakutin, M. V., Yttri, K. E., and Hüglin, C.: Ice Nucleating Particle Concentrations Increase When Leaves Fall in Autumn, Atmosphere-Basel, 8, 202, https://doi.org/10.3390/atmos8100202, 2017.

Cozic, J., Mertes, S., Verheggen, B., Cziczo, D. J., Gallavardin, S. J., Walter, S., Baltensperger, U., and Weingartner, E.: Black carbon enrichment in atmospheric ice particle residuals

observed in lower tropospheric mixed phase clouds, J Geophys Res-Atmos, 113, 11, https://doi.org/10.1029/2007jd009266, 2008.
Hill, T. C. J., DeMott, P. J., Tobo, Y., Fröhlich-Nowoisky, J., Moffett, B. F., Franc, G. D., and Kreidenweis, S. M.: Sources of organic ice nucleating particles in soils, Atmos. Chem. Phys., 16, 7195-7211, 10.5194/acp-16-7195-2016, 2016.
Huang, S., Hu, W., Chen, J., Wu, Z., Zhang, D., and Fu, P.: Overview of biological ice nucleating particles in the atmosphere, Environment International, 146, 106197, https://doi.org/10.1016/j.envint.2020.106197, 2021.
Jiang, H., Yin, Y., Su, H., Shan, Y. P., and Gao, R. J.: The characteristics of atmospheric ice nuclei measured at the top of Huangshan (the Yellow Mountains) in Southeast China using a newly built static vacuum water vapor diffusion chamber, Atmos Res, 153, 200-208, https://doi.org/10.1016/j.atmosres.2014.08.015, 2015.
Kunert, A. T., Pöhlker, M. L., Tang, K., Krevert, C. S., Wieder, C., Speth, K. R., Hanson, L. E., Morris, C. E., Schmale Iii, D. G., Pöschl, U., and Fröhlich-Nowoisky, J.: Macromolecular fungal ice nuclei in Fusarium: effects of physical and chemical processing, Biogeosciences, 16, 4647-4659, https://doi.org/10.5194/bg-16-4647-2019, 2019.
Levin, E. J. T., McMeeking, G. R., DeMott, P. J., McCluskey, C. S., Carrico, C. M., Nakao, S., Jayarathne, T., Stone, E. A., Stockwell, C. E., Yokelson, R. J., and Kreidenweis, S. M.: Ice-nucleating particle emissions from biomass combustion and the potential importance of soot aerosol, J Geophys Res-Atmos, 121, 5888-5903, https://doi.org/10.1002/2016jd024879, 2016.
Murray, B. J., O'Sullivan, D., Atkinson, J. D., and Webb, M. E.: Ice nucleation by particles immersed in supercooled cloud droplets, Chem. Soc. Rev., 41, 6519-6554, https://doi.org/10.1039/c2cs35200a, 2012.
O'Sullivan, D., Murray, B. J., Malkin, T. L., Whale, T. F., Umo, N. S., Atkinson, J. D., Price, H. C., Baustian, K. J., Browse, J., and Webb, M. E.: Ice nucleation by fertile soil dusts: relative importance of mineral and biogenic components, Atmos. Chem. Phys., 14, 1853-1867, https://doi.org/10.5194/acp-14-1853-2014, 2014.
Petters, M. D. and Wright, T. P.: Revisiting ice nucleation from precipitation samples, Geophys Res Lett, 42, 8758-8766, https://doi.org/10.1002/2015GL065733, 2015.
Phelps, P., Giddings, T. H., Prochoda, M., and Fall, R.: Release of cell-free ice nuclei by Erwinia herbicola, Journal of Bacteriology, 167, 496-502, https://doi.org/10.1128/jb.167.2.496-502.1986, 1986.
Schrod, J., Weber, D., Drucke, J., Keleshis, C., Pikridas, M., Ebert, M., Cvetkovic, B., Nickovic, S., Marinou, E., Baars, H., Ansmann, A., Vrekoussis, M., Mihalopoulos, N., Sciare, J., Curtius, J., and Bingemer, H. G.: Ice nucleating particles over the Eastern Mediterranean measured by unmanned aircraft systems, Atmos Chem Phys, 17, 4817-4835, https://doi.org/10.5194/acp-17-4817-2017, 2017.

Measurement report: Atmospheric Ice Nuclei at Changbai Mountain (2623 m a.s.l.) in Northeastern Asia

Yue Sun[1], Yujiao Zhu[1], Yanbin Qi[2], Lanxiadi Chen[3], Jiangshan Mu[1], Ye Shan[1], Yu Yang[1], Yanqiu Nie[1], Ping Liu[1], Can Cui[1], Ji Zhang[1], Mingxuan Liu[1], Lingli Zhang[4], Yufei Wang[2], Xinfeng Wang[1], Mingjin Tang[3], Wenxing Wang[1], Likun Xue[1]

[1]Environment Research Institute, Shandong University, Qingdao 266237, China
[2]Jilin Provincial Technology Center for Meteorological Disaster Prevention, Changchun 130062, China
[3]State Key Laboratory of Organic Geochemistry, Guangzhou Institute of Geochemistry, Chinese Academy of Sciences, Guangzhou 510640, China
[4]Changbai Mountain Meteorological Observatory, An Tu, Jilin 133613, China

Correspondence to: Yujiao Zhu (zhuyujiao@sdu.edu.cn), Likun Xue (xuelikun@sdu.edu.cn)

Abstract. Atmospheric ice nucleation plays an important role in modulating the global hydrological cycle and atmospheric radiation balance. To date, few comprehensive field observations of ice nuclei have been carried out at high-altitude sites, which is close to the height of mixed-phase cloud formation. In this study, we measured the concentrations of ice-nucleating particles (INPs) in the immersion freezing mode at the summit of Changbai Mountain (2623 m above sea level), Northeast Asia, in summer 2021. The cumulative number concentration of INPs varied from 1.6×10^{-3} L−1 to 78.3 L^{-1} over the temperature range from −29.0 ℃ to −5.5 ℃. Proteinaceous-based biological materials accounted for the majority of INPs, with the proportion of biological INPs (bio-INPs) exceeding 67% across the entire freezing temperature range, with this proportion even exceeding 90% above −13.0 ℃. At freezing temperatures ranging from −11.0 ℃ to −8.0 ℃, bio-INPs were found to significantly correlate with wind speed (r = 0.5-0.8, $p < 0.05$) and Ca^{2+} (r = 0.6-0.9), and good but not significant correlate with isoprene (r = 0.6-0.7) and its oxidation products (isoprene × O_3) (r = 0.7), suggesting that biological aerosols may attach to soil dust surfaces and contribute to INPs. During the daytime, bio-INPs showed a positive correlation with the planetary boundary layer height at freezing temperatures ranging from −22.0 ℃ to −19.5 ℃ ($r > 0.7$, $p < 0.05$), with the valley breezes from southern mountainous regions also influencing the concentration of INPs. Moreover, the long-distance transport of air mass from the Japan Sea and South Korea significantly contributed to the high concentrations of bio-INPs. Our study emphasizes the important role of biological sources of INPs in the high-altitude atmosphere of northeastern Asia, as well as the significant contribution of long-range transport to the INP concentrations in this region.

1 Introduction

Clouds play a crucial role in regulating the Earth's energy balance by absorbing, reflecting, and scattering solar and terrestrial radiation (Zhou et al., 2016; Bjordal et al., 2020). Global precipitation is predominantly produced by clouds containing the ice phase, especially in continental regions and mid-latitude oceans, emphasizing the paramount significance of investigating ice formation within clouds (Mulmenstadt et al., 2015; Lau and Wu, 2003; Demott et al., 2010; Kanji et al.,

2017). Atmospheric aerosols can act as ice-nucleating particles (INPs), triggering the freezing of cloud droplets through heterogeneous nucleation processes (Rinaldi et al., 2017; Koop et al., 2000; Rosenfeld and Woodley, 2000; Demott et al., 2003; Cziczo et al., 2013; Murray et al., 2010). Currently, the four main mechanisms of heterogeneous ice nucleation are considered: deposition nucleation, condensation freezing, immersion freezing, and contact freezing (Demott et al., 2003; Vali et al., 2015). Recent studies have concluded that water saturation is a prerequisite for ice formation in mixed-phase clouds, and that contact and immersion freezing are the most primary pathways for ice formation (Sassen and Khvorostyanov, 2008; Phillips et al., 2007; Murray et al., 2012).

Various aerosol particles are potential INPs, such as biological aerosols (Pratt et al., 2009; Tobo et al., 2013), mineral dusts (Pratt et al., 2009; Atkinson et al., 2013), sea spray aerosols (Mccluskey et al., 2017; Alpert et al., 2022), carbonaceous aerosols (Grawe et al., 2018; Demott, 1990; Diehl and Mitra, 1998; Fornea et al., 2009), volcanic ashes (Grawe et al., 2016; Umo et al., 2015). Biological aerosols such as microbial and proteinaceous origin, containing proteins in cell-free macromolecules or intact cell membranes, demonstrate significant efficiency as INPs at temperatures above −15 ℃ (Phelps et al., 1986; Petters and Wright, 2015; Murray et al., 2012; Kunert et al., 2019; Huang et al., 2021). For example, lichens can induce freezing above −10 ℃ (Moffett et al., 2015), and some bacterial organisms like *Pseudomonas syringae* can facilitate droplet freezing at extremely high temperatures (above −2 ℃) (Maki et al., 1974). For the non-proteinaceous biological particles, such as pollen, cellulose, and other macromolecular organic particles, can also induce ice formation through heat-resistant polysaccharides on their surfaces, but at lower temperatures than proteinaceous biological particles (Knopf et al., 2010; Pummer et al., 2012). Mineral dust and sea spray aerosols predominantly consist of inorganic compounds and serve as effective INPs at temperatures below -15°C. The ice-nucleating properties of aerosols are affected by many factors. For instance, the size of particles is a crucial factor for providing active sites for ice formation, with larger particles containing more efficient ice nucleation sites than smaller ones (Chen et al., 2018; Demott et al., 2010; Demott et al., 2015). In addition, the chemical composition and surface properties of aerosol particles, such as their surface topology, defects, roughness, and functional groups, also influence their activity as INPs (Freedman, 2015; Kanji and Abbattt, 2010; Mahrt et al., 2018; Roudsari et al., 2022). Furthermore, the ice-nucleating properties of aerosol particles can be modified through chemical reactions with trace gases or organic/inorganic component or through physical processes such as efflorescence or deliquescence (Cziczo et al., 2009; Hoose and Möhler, 2012; Creamean et al., 2013; Tang et al., 2016; Tang et al., 2018).

Over recent decades, numerous studies have focused on investigating heterogeneous ice nucleation in various atmosphere environments. In low-altitude atmospheres, the abundance of ground-based sources and sinks results in spatial distribution heterogeneity, which restricts the characterization of INPs properties on a regional scale. At present, there remain uncertainties how INPs can be extended and transported to the altitudes of mixed-phase cloud formation (approximately 3–7 km). High-altitude sites provide favourable conditions for in situ observations to investigate INPs characteristics, as they can represent tropospheric background conditions and reflect long-distance transport and vertical mixing processes prior to arriving at the ground sampling site. Therefore, field experiments have been conducted in several high-altitude sites. For example, in the

Switzerland, simultaneous measurements taken at different-altitude stations revealed a reduction of approximately 50% per kilometer in the abundance of INPs in the vertical gradient (ranging from 489 m above sea level (a.s.l.) to 3580 m a.s.l. in the Swiss Alps) in the warm season (Conen et al., 2017). This decline in INPs could exceed 60% per kilometer during the cold season (from 1631 m a.s.l. to 2693 m a.s.l.) (Wieder et al., 2022), which was attributed to the scarcity of effective INPs sources in high-altitude atmosphere. Note that variations in sampling methods and the influence of wind directions can also exert an impact on INP concentrations. In contrast, Schrod et al. (2017) reported an increase in INPs abundance of approximately 10 times over the eastern Mediterranean (2500 m a.s.l.) relative to ground level using unmanned aircraft systems, with this difference attributed to the long-distance transport of a series of elevated Saharan dust plumes at the height of a few kilometers. In mountainous areas with high vegetation coverage, biogenic aerosols are the most abundant type of INPs. For example, at the Jungfraujoch station (3580 m a.s.l.) in the Swiss Alps, approximately 80% of INPs were biological aerosols at freezing temperatures above −15 ℃ under free-tropospheric conditions (Conen et al., 2022). Similarly, at the Puy de Dôme station (1465 m a.s.l.) in France, the average contribution of biological aerosols in cloud water could reach up to 85% at freezing temperatures above −10 ℃ (Joly et al., 2014). To date, fewer field observations have been carried out in high-altitude regions in China. For example, Jiang et al. (2014, 2015) performed measurements at Mt. Huangshan (1840 m a.s.l.) in Southeast China, finding that larger particles were more likely to be effective INPs. Lu et al. (2016) collected seven rainwater samples from three mountains in eastern China, i.e., Changbai Mountain (at the peak of 2740 m a.s.l.), Wuling Mountain (900 m a.s.l.), Dinghu Mountain (1000 m a.s.l.), and found that the initiated freezing temperature was approximately −6 ℃, but bacteria played minor roles in the overall INP activity. Because the number of rainwater samples was limited, further research is necessary to explore the impact of biological INPs on cloud droplets and their contribution to the formation of precipitation.

In this study, we conducted offline INP measurements at the top of Changbai Mountain (2623 m a.s.l.) in Jilin province, China, which is located in Northeast Asia. This region is particularly vulnerable to climate change because of the presence of distinct ecotones caused by land type changes, as well as the influence of the North Atlantic Oscillation and the Northern Hemisphere circulation (Sugita et al., 2007; Zhang et al., 2021). Moreover, Northeast Asia is densely populated and serves as a crucial breadbasket for the world, making rainfall an essential factor for determining crop yields. Given the high altitude of Changbai Mountain, it is an ideal location to capture the characteristics of the regional atmospheric background and transboundary transport of air mass. Our main objective was to investigate the concentration levels of INPs and identify their major sources at the height of the mountain's peak. Additionally, we evaluated the impact of the planetary boundary layer (PBL) height, valley breezes, and transport pathways of INPs to gain a better understanding of INPs sources in this region. Our findings could provide valuable insights into the formation and behaviour of clouds over this region.

2 Methods

2.1 Site description

Changbai Mountain is the highest mountain in the border region between China and the Korean Peninsula. It is situated on the transport pathways of continental air pollutants from Asia to the North Pacific Ocean and even as far as the Arctic. The regional topography is characterized by forests and mountains, with elevations ranging from 410 m a.s.l. to 2740 m a.s.l. The southeast exhibits higher elevations compared to the northwest (Wang et al., 2014). At the top of Changbai Mountain, there is a vast crater known as Tianchi Lake, which has a depth of 373 m and covers an area of 9.82 km^2. In this study, a field campaign was carried out at the Tianchi Meteorological Station (Tianchi Site, 42.03°N, 128.08°E, 2623 m a.s.l., Figure 1), which is approximately 410 m north of Tianchi Lake, from July 24 to August 24, 2021.

Changbai Mountain is situated within the westerly wind belt and experiences a typical temperate continental mountain climate influenced by the monsoon, characterized by long cold winters and short temperate summers. The prevailing winds in this region are the westerly and northwesterly winds in the spring, autumn, and winter season and the southeasterly and southwesterly winds in the summer season (Zhao et al., 2015). The annual average temperature is typically lower than −7.4 ℃ (Jin et al., 2018), with the mountain summit always covered by snow and ice for approximately three quarters of the year. Figure S1 presents the timeseries of meteorological parameter, NOx concentration, and the of INP concentrations during the field measurements. During the campaign, the relative humidity (RH) ranged from 33% to 100%, with a mean of 92.4 ± 11.8%. Notably, seventy percent of the RH exceeded 90% throughout the campaign, indicating that the campaign was performed under humid weather conditions. The sampling site was predominantly affected by southerly and westerly winds, with wind speed (WS) ranging from 0.1 m s^{-1} to 25.7 m s^{-1}. Changbai Mountain is a national nature reserve with no large industrial facilities nearby, and tourism is the important economic activity in the region. Due to the emergence of novel coronavirus (COVID-19) cases, strict lockdown measures have been implemented from August 10, 2021, resulting in a substantial reduction in visitor numbers, as indicated by the marked decrease in NOx concentration (Figure S1). The surroundings of the observation site are covered by dense vegetation, such as shrubs and perennial herbs. Most of the time, the site is above the PBL and in the free troposphere, making it an ideal site for studying the regional background atmosphere of Northeast Asia.

2.2 Sample collection

Bulk aerosol particles were collected on polycarbonate (PCTE) membrane filters (Sterlitech 1870, nominal porosity 0.45 μm) using a TH-150D medium flow sampler (Wuhan Tianhong Corporation, China, Figure 1c) at a flow rate of 50 L min^{-1} for the INPs analysis. Samples were collected during the daytime (06:00 to 17:30) and nighttime (18:00 to 05:00 in the following day) in local time. A total of 24 PCTE filters were collected, including 22 aerosol samples and 2 blank filters. These samples were used for INP analysis and detailed sampling information is provided in Table S1. Meanwhile, fine particulate matter ($PM_{2.5}$) samples were collected on quartz microfiber filters (PALL Pallflex, 7204), which were heated at 560 ℃ for 4 h before sampling to remove any adsorbed organics, using another medium flow sampler (Wuhan Tianhong Corporation,

China) with a 2.5 μm impactor at a flow rate of 100 L min^{-1}. A total of 157 samples were collected on quartz filters every 3 h and used for chemical composition analysis. After sampling, all filter samples were kept frozen at ≤ −18 ℃ until analysis.

Real-time measurements of $PM_{2.5}$ and black carbon (BC) were recorded at 1 min intervals by using SHARP 5012 (Thermo Scientific, USA) and SHARP 5030 (Thermo Scientific, USA), respectively. Trace gases including CO, SO_2, NO_x, and O_3, were detected using Thermo Scientific 48i, 43i, 42i, and 49i, respectively. Ambient volatile organic compounds (VOCs) were collected by taking air samples using stainless-steel canisters at two specific time intervals (i.e., 11:00-13:00 and 20:00-22:00) on clean days, and the sampling frequency increased to every 3 h during air pollution episodes. Meteorological data, such as temperature, humidity, WS, wind direction, pressure, and precipitation, were monitored by the Tianchi weather station, a national meteorological station located approximately 20 m from the sampling site.

2.3 INPs analysis

INP measurements in the immersion mode were conducted using the Guangzhou Institute of Geochemistry Ice Nucleation Apparatus (GIGINA) from −40 ℃ to 0 ℃. GIGINA is a cold-stage-based ice nucleation array that consists of a commercial cold stage, an enclosed droplet chamber (LTS120, Linkam, Epsom Downs, UK), an external refrigerated water circulator (VIVO RT4, Julabo, Seelbach, Germany), a charge-coupled device (CCD) camera (DMK33G274, The Imaging Source, Bremen, Germany), a ring LED light, and a computer system. Further details regarding GIGINA have been published by Chen et al. (2023).

Each polycarbonate filter was immersed in 5 mL MilliQ water (resistivity of 18.2 MΩ cm^{-1} at 25 ℃) and sonicated for 30 min to wash off particles (Chen et al., 2021). Note that an ice water bath was utilized during ultrasonic extraction to mitigate any potential alterations in protein properties and biogenic activities. In addition, the suspension underwent dilution at multiple levels: 30-fold, 60-fold, and 120-fold, in order to generate spectra that encompass freezing temperature below -25°C, as illustrated in Figure S3. The INPs measurement process is briefly described as follows. First, a hydrophobic glass slide was placed on a cold stage and filled with silicone oil to achieve good thermal contact. Second, a round aluminum spacer with 90 round compartments was placed on the glass slide, and the particle suspension was sequentially pipetted into each compartment. Then, another glass slide was placed above the spacer to avoid the Wegener–Bergeron–Findeisen process (Jung et al., 2012). Afterward, the temperature of the droplets was cooled down to 0 ℃ at a cooling rate of 10 ℃ min^{-1}, after which the cooling of the droplets continued at a rate of 1 ℃ min^{-1} until all the droplets were frozen. During the freezing experiment, high-purity nitrogen was continuously delivered onto the cold stage to prevent frost from forming on the surface of the glass slide. Meanwhile, real-time images of the droplets were photographed by the CCD camera and recorded by the LINK software every 6 s. After the experiment, the phase transition of each droplet was identified by analyzing the changes in image brightness, which distinguished between unfrozen (white) and frozen (dark) droplets.

The frozen fraction, $f_{ice,}$ was calculated according to Eq. (1):

$$f_{ice}(T) = \frac{n_{ice}}{n_{tot}} \ , \tag{1}$$

where n_{ice} is the number of frozen droplets at a certain temperature T, and n_{tot} is the total number of droplets (90 droplets). The cumulative concentration of each droplet above K (T), and the cumulative number concentration of INPs (N_{INP}) in the unit volume of sampled air, were calculated following the method of Vali (1971, 2015):

$$K(T) = -\frac{ln[1-f_{ice}(T)]}{V}(cm^{-3}\ of\ water) \ , \tag{2}$$

$$N_{INP}(T) = -\frac{ln[1-f_{ice}(T)]}{V_{air}}(L^{-1}\ air), \tag{3}$$

where V is the volume of each droplet (1 µL), and V_{air} is the total volume of sampled air per droplet converted to standard conditions (0 ℃ and 1013 hPa). In our study, the N_{INP} values were significantly larger in filter samples than in the field blanks. The rarity of INPs in the atmosphere leads to their low concentration in the suspension. Because the suspension used in the measurement contained a limited number of droplets, we need to consider the resulting uncertainty for estimating N_{INP} in both the whole suspension and thus the atmosphere. Additionally, the uncertainty associated with the droplet-freezing apparatus cannot be ignored. To address these uncertainties, we calculated the confidence intervals of the apparatus for f_{ice} according to the method of Gong et al. (2022) and Agresti and Coull (1998):

$$\left(f_{ice} + \frac{Z_{\alpha/2}^2}{2n_{tot}} \pm Z_{\propto/2}\sqrt{[f_{ice}(1-f_{ice}) + Z_{\alpha/2}^2/(4n_{tot})]/n_{tot}}\right) /\left(1 + Z_{\alpha/2}^2/n_{tot}\right), \tag{4}$$

where $Z_{\alpha/2}$ is the standard score at a confidence level $\boldsymbol{\alpha}/2$, for which the 95% confidence interval is 1.96.

2.4 Chemical analysis

The $PM_{2.5}$ samples collected by quartz membranes were used to analyze the particle chemical composition. For each sample, an eighth of the filter was ultrasonically extracted using 15 mL MilliQ water for 30 min to make a suspension. The concentrations of inorganic water-soluble anions (Cl^-, SO_4^{2-}, and NO_3^-) and cations (Na^+, NH_4^+, K^+, Mg^{2+}, and Ca^{2+}) were identified using the ICS 1100 ion chromatograph (Thermo Scientific). In addition, the concentrations of organic carbon (OC) and elemental carbon (EC) were measured using the Sunset Laboratory Model-5 semi-continuous OC/EC field analyzer. The VOCs canister samples were analyzed using online gas chromatography–mass spectrometry (TT24xr, Makers, UK; GC–MS, Thermo Scientific, USA) in the laboratory. A total of 106 target VOCs, including 29 alkanes, 11 alkenes, one alkyne, 17 aromatics, 35 halogenated hydrocarbons and 13 oxygenated VOCs (OVOCs), were quantified.

2.5 The PBL data and air mass back trajectory model

The PBL data were downloaded from the fifth-generation ECMWF global atmospheric reanalysis product (ERA5 https://cds.climate.copernicus.eu), which provides hourly records on latitude–longitude grids at 0.25° × 0.25° resolution. The 72-h air mass backward trajectories at the sampling site were calculated on an hourly basis during our sampling days. These

calculations were performed using the Hybrid Single Particle Lagrangian Integrated Trajectory (HYSPLIT) model (http://ready.arl.noaa.gov/HYSPLIT.php), which is developed by the National Oceanic and Atmospheric Administration Air Resources Laboratory (NOAA ARL) (Stein et al., 2015). The simulations were based on meteorological data from the Global Data Assimilation System (GDAS) with a spatial resolution of 1° × 1° and an end altitude of the backward trajectory of 2623 m a.s.l. Using the open-source software of MeteoInfo, concentration-weighted trajectory (CWT) analysis was conducted to explore the potential sources of INPs based on the air mass backward trajectories and N_{INP}. The CWT assigns the average weighted concentration by trajectories were divided into grids. The calculation was used Equation 5 according to the method of Hsu et al. (2003):

$$C_{ij} = \frac{1}{\sum_{k=1}^{M} \tau_{ijk}} \sum_{k=1}^{M} C_k \tau_{ijk}, \quad (5)$$

where C_{ij} is the average weighted concentration in the ij cell, k is the index of the trajectory, M is the total number of trajectories, C_k is the concentration observed on arrival of trajectory k in the ij cell, and τ_{ijk} is the time spent in the ij cell by trajectory. The weight function W_{ij} was also applied to the CWT analysis to reduce the uncertainty in the cells with small values of n_{ij}:

$$WCWT_{ij} = C_{ij} \times W(n_{ij}), \quad (6)$$

Note that uncertainty may exist in the CWT analysis due to the relatively small dataset of INPs in this study.

3 Results and Discussion

3.1 INP concentrations

A metric was applied to evaluate the freezing of droplets, i.e., the freezing temperature at which 50% of the droplets are frozen (T_{50}). The frozen fractions (f_{ice}) of all freezing curves containing the collected samples and MilliQ water are shown in Figure 2a and Figure S2. The T_{50} of MilliQ water ranged from −30.0 ℃ to −26.0 ℃, reflecting the low background value of the droplet-freezing apparatus. For the blank filters, T_{50} was averaged to −24.2 ± 2.1 ℃, which was slightly higher than that of MilliQ water, but significantly lower than that of the collected samples (for which T_{50} was −17.0 ± 4.1 ℃). This result suggests the presence of minimal contaminants stemming from the filter membrane. In the following analysis, the concentrations of the two blank filters were subtracted from the daytime and nighttime samples at each freezing temperature, respectively.

The N_{INP} values as a function of temperature are presented in Figure 2b, where the pink and blue circles represent the samples collected during the daytime and nighttime, respectively. The freezing of ambient samples was observed in the temperature range of −29.0 ℃ to −5.5 ℃, with N_{INP} spanning three orders of magnitude from 1.6×10^{-3} L^{-1} to 78.3 L^{-1}. For freezing temperatures above T_{50} (−17.0 ℃), the temperature region is referred to as the high-temperature region (HTR), where N_{INP} spans three orders of magnitude from 1.6×10^{-3} L^{-1} to 6.2 L^{-1}. Some of the N_{INP} curves exhibited bumps in the HTR,

which has been also observed at a coastal site (the Cape Verde Atmospheric Observatory, Africa) by Welti et al. (2018) in air samples and in the upper bound of the composite nucleus spectrum of cloud water and precipitation samples by Petters and Wright (2015). Welti et al. (2018) reported that the narrower the IN properties, the steeper slope can be observed in a temperature spectrum. In contrast, in the low-temperature region (LTR, freezing temperature below T_{50}, -17.0 ℃ ~ -29.0 ℃), N_{INP} showed a relatively narrow variation from 0.1 L^{-1} to 78.3 L^{-1}. Furthermore, there were no significant differences observed in N_{INP} between daytime and nighttime (the significance level is 0.61). However, in some mountainous sites, such as Mt. Huang, where samples were collected twice daily at 08:00 and 14:00 (Jiang et al., 2015), and the Weissfluhjoch in the Swiss Alps, where samples were collected at 20-minute intervals (Wieder et al., 2022), N_{INP} displayed a distinct diurnal cycle induced by the orographically lifted air masses containing high INP concentrations from low elevation upstream during the daytime. In this study, we collected two samples per day, and the limited dataset size and low sampling frequency may have contributed to the absence of diurnal variations.

We compared our N_{INP} measurements with previous results from diverse sites. For instance, in mountainous regions, the N_{INP} value at the Weissfluhjoch varied from 10^{-4} to 10^{1} in the temperature range of −24.0 ℃ to −4.0 ℃ (Wieder et al., 2022). In our observations, the spectra range of N_{INP} were narrowly located in the relatively high-concentration regions at overlapping freezing temperatures compared to the measurements of Wieder et al. (2022). Jiang et al. (2015) reported that the INP concentrations at the top of Mt. Huang spanning from 0.1 L^{-1} to 11.9 L^{-1} over a temperature range from -15.0 ℃ to -23.0 ℃, which overlapped with our results. In the LTR, our results were comparable to the measurements conducted at the Storm Peak Laboratory in the northwestern Colorado Rocky Mountains by Hodshire et al. (2022). But in HTR, Conen et al. (2022) recorded results in Switzerland were 1-3 orders of magnitude higher than our study, and its aerosolized epiphytic microorganisms contributed most of the INPs to primary ice formation at Jungfraujoch. Gong et al. (2022) measured INPs at the mountain station at Cerro Mirador (622 m a.s.l., Chile), and reported N_{INP} values lower than those in our study by around one order of magnitude during the measured freezing temperatures (from −26.0 ℃ to −3.0 ℃). In heavily polluted urban sites, such as Beijing (Chen et al., 2018) and Tai'an (Jiang et al., 2020) in China, the INP concentrations were comparable to our measurements at overlapping freezing temperatures. Chen et al., (2018) reported that INP concentrations might not be influenced by urban air pollution because no correlation was found between the immersion-freezing nuclei concentration and the $PM_{2.5}$ or BC concentration. Carbonaceous particles might not act as efficient INPs in the immersion mode or may decrease ice nucleation activity because of the formation of organic coatings in polluted urban environments with complex aerosol sources (Schill et al., 2020; Nichman et al., 2019; Hammer et al., 2018).

3.2 Contribution of biological particles, other organics, and inorganics to INPs

Generally, biological particles can induce ice nucleation in the immersion mode at relatively high temperatures above −15.0 ℃ (Murray et al., 2012). Proteinaceous components mainly induce biological ice nucleation, and wet heat treatment (i.e., heating the particle suspension to 95.0 ℃ for 30 min) is used to identify the protein-based biological ice nucleation

activity (Beall et al., 2022; Chen et al., 2021). We measured the N_{INP} values of the suspensions after heat treatment, which we refer to as heat-resistant N_{INP} ($N_{INP\text{-}heat}$, as shown in Figure S3), and the difference between the original N_{INP} and $N_{INP\text{-}heat}$ was considered to be mainly due to the proteinaceous biological N_{INP} ($N_{INP\text{-}bio}$). However, some biological aerosols, such as pollen, cellulose, or other macromolecular organic particles, are insensitive to heat treatment at 95.0 ℃ (Daily et al., 2022). Therefore, we also measured the heat-stable organic INPs, which are defined as other organic INPs (other org-INPs), following the methods of Suski et al. (2018) and Testa et al. (2021). We added 30% H_2O_2 (guaranteed reagent) to the suspension to obtain a final concentration of 10%, and then heated it at 95 ℃ for 20 min under UVB fluorescent bulbs. To prevent freezing point depression, we neutralized the remaining H_2O_2 in the suspension with catalase. The N_{INP} value following treatment by this procedure was denoted H_2O_2-resistant N_{INP} ($N_{INP\text{-}H2O2}$), which is the concentration of inorganic INPs ($N_{INP\text{-}inorg}$). The difference between heat-resistant N_{INP} and H_2O_2-resistant N_{INP} was considered to be equivalent to the concentration of other organic INPs ($N_{INP\text{-}other\ org}$).

Figure 3 illustrates the concentrations and fractions of the three types of INPs. The biological INPs (bio-INPs) showed ice nucleation activity at temperatures between −28.5 ℃ and −5.5 ℃. After the ice nucleation activity of the bio-INPs was destroyed, $N_{INP\text{-}heat}$ decreased by around 1–2 orders of magnitude compared with the original N_{INP}, indicating a significant contribution of $N_{INP\text{-}bio}$, as shown in Figure S3. The initial freezing temperature of other org-INPs was −11.0 ℃, which was approximately 5.5 ℃ lower than that of bio-INPs. Inorganic INPs exhibited ice nucleation activity at temperatures between −28.0 ℃ and −10.0 ℃. Interestingly, the initial freezing temperatures of some inorganic INPs were slightly higher than those of other org-INPs, indicating that some inorganic aerosols could trigger freezing at relatively high temperatures.

The proportions of the three types of INPs as functions of temperature are presented in Figure 3(b). Here, the fractions of $N_{INP\text{-}bio}$ ($F_{INP\text{-}bio}$) account for 100% of the N_{INP} value above −11 ℃, and show a decreasing trend as the temperature decreases from −11.5 ℃ to −16.5 ℃. This decreasing trend of $F_{INP\text{-}bio}$ is consistent with trends observed in other areas dominated by bio-INPs in similar temperature regions (Gong et al., 2022; O'sullivan et al., 2018; Testa et al., 2021), suggesting that the importance of bio-INPs decreases with decreasing temperature. Interestingly, when the temperature decreased from −16.5 ℃ to −21.5 ℃, the median of $F_{INP\text{-}bio}$ increased from 0.8 to 0.9, indicating the presence of bio-INPs with relatively high ice-nucleating activity in the LTR. Previous observational studies have indicated that although most bio-INPs act as ice nuclei at high freezing temperature, some heat-sensitive biological aerosols, such as fungal cloths, exhibit ice-nucleating activity at low temperatures (Iannone et al., 2011; Kanji et al., 2017). Modelling studies have also shown that bio-INPs can influence the ice phase of clouds and produce ice crystals when the cloud-top temperature is below −15 ℃ (Hummel et al., 2018). This phenomenon may also be related to the sensitivity of different species of biological aerosol to heating conditions. In wet heat treatment it is assumed that the ice-nucleating active protein in bio-INPs is completely destroyed and denatured, thus losing any ice formation potential. However, this method may lead to decrease in the freezing temperature of bacteria and fungi, but their ice-forming activity still cannot be ignored (Daily et al., 2022). As the temperature dropped to -25.0 ℃, $F_{INP\text{-}bio}$ began to decrease significantly to 0.7. Overall, the median value of $F_{INP\text{-}bio}$ was more than 67% in the entire temperature range from

−25.0 ℃ to −5.5 ℃, with the value exceeding 90% above −13.0 ℃, which was much higher than in some mountainous areas in southwestern South America (Gong et al., 2022) and urban areas in China (Chen et al., 2021). The fractions of $N_{\text{INP-other org}}$ ($F_{\text{INP-other org}}$) showed an opposite trend from that of $F_{\text{INP-bio}}$ at freezing temperatures between −25.0 ℃ and −11.0 ℃. First, $F_{\text{INP-other org}}$ increased from 0.08 to 0.2 as the temperature decreased from −11.0 ℃ to −15.0 ℃, and then sharply decreased from 0.2 to 0.05 as the temperature decreased further from −15.0 ℃ to −22.0 ℃. When the temperature was lower than -22.0 ℃, $F_{\text{INP-other org}}$ gradually increased to 0.3. The fractions of $N_{\text{INP-inorg}}$ ($F_{\text{INP-inorg}}$) remained below 0.22 throughout the entire temperature range, with an increasing trend observed below -22.0 ℃, which is consistent with previous studies in some clean atmospheres. Overall, our results showed that protein-based biological aerosols contribute the most to INPs at Changbai Mountain.

3.3 Source analysis of different types of INPs

We investigated the relationship between different types of INPs and various environmental conditions, as well as the gases and particle compositions, as show in Figure 4 (details can be found in Table S2). In the HTR, our results showed a significant positive correlation (r = 0.5-0.8, p < 0.05) between N_{INP} and WS with temperature range from −11. 0 ℃ to −9.0 ℃. High WS can enhance the uplift of soil dust and the long-distance transport of aerosols. Moreover, N_{INP} and Ca^{2+} showed a good positive correlation (r = 0.6-0.9) within the range of -11.0 ℃ to -8.0 ℃, leading us to speculate that soil dust may play an important role in ice nucleation in this temperature range. Previous studies have shown that when soil dusts mix with biological components, their freezing temperatures can increase to as high as −6 ℃, which is much higher than that of natural dust (below −20 ℃) (Hill et al. 2016; O'sullivan et al., 2014). In the LTR, N_{INP} demonstrated a significant positive correlation with temperature (r = 0.5-0.6, p < 0.05) and a significant negative correlation with RH (r = 0.6-0.7, p < 0.05). When the temperature falls below -20.0 ℃, N_{INP} exhibits a significant positive correlation with $PM_{2.5}$ and BC, implying that inorganic components may serve as active INPs in lower freezing temperature.

We also investigated the potential sources of different types of INPs, as shown in Figure 4(b–d). Similar to the total INPs, $N_{\text{INP-bio}}$ were more abundant during the high temperature and low RH. And a significant positive correlation was showed between $N_{\text{INP-bio}}$ with WS (r = 0.5-0.7) and Ca^{2+} (r = 0.6-0.9) at temperatures ranging from −11 ℃ to −8 ℃, as well as good but not significant positive correlation with isoprene (r = 0.6-0.7, p > 0.05) and its oxidation products (isoprene × O_3, r = 0.7, p > 0.05). O'sullivan et al. (2016) and Augustin-Bauditz et al. (2016) reported that biological materials may attach to or mix with dust particles and promote INPs formation. However, no mineral dust events were observed during our sampling period, based on the low mass concentrations of $PM_{2.5}$ (the range from 1.5 μg m^{-3} to 31.6 μg m^{-3} with average of 9.3±6.0 μg m^{-3}) and metal ions with Ca^{2+} (the range from 0.007 μg m^{-3} to 3.6 μg m^{-3} with average of 0.5 ± 1.0 μg m^{-3}). We speculate that the source of bio-INPs was related to soil dust. The higher WS may have facilitated the exposure of the local soil dust and bioaerosol containing bio-INPs to the air. Alternatively, the long-distance transport of biological aerosol attached to soil dust surfaces may also contribute to bio-INPs, leading to the high N_{INP} accompanied by high WS and Ca^{2+}.

However, we did observe that $N_{INP\text{-}other\ org}$ exhibited positive correlations with temperature and negative correlations with WS, indicating that these particles have local sources. At temperatures ranging from −16.0 ℃ to −14.0 ℃, $N_{INP\text{-}other\ org}$ showed a positive correlation with isoprene (r = 0.7-0.8, p < 0.05), which is considered to be an important natural gaseous precursor to the formation of secondary organic aerosols. Additionally, $N_{INP\text{-}other\ org}$ was positively correlated with the oxidation of isoprene bio-INPs (r = 0.5-0.6) at temperatures ranging from −18.0 ℃ to −14.0 ℃, although this correlation was not significant. We hypothesize that the formation of secondary organic aerosols was the main source of other org-INPs.

In the temperature range of -23.0 ℃ to -17.0 ℃ within the LTR, $N_{INP\text{-}inorg}$ exhibited a significant negative correlation with RH (r = 0.5-0.7, p < 0.05), indicating an enrichment of inorg-INPs under low RH conditions. $N_{INP\text{-}inorg}$ showed a significant positive correlation with BC and SNA in the LTR. BC-containing particles resulting from anthropogenic activities have been speculated to play a role in INPs formation (Cozic et al., 2008; Levin et al., 2016). Note that $PM_{2.5}$ chemical composition was used in this study, which may lead to uncertainties in the interpretation of the bulk IN activities.

3.4 Transport pathways of INPs

At the mountaintop site, the horizontal and vertical transport of air mass are important pathways for INPs under favorable conditions, such as valley breezes, variations in mixing layer height, and long-range transport processes (Chow et al., 2013; Wieder et al., 2022). Understanding the coupling between the PBL changes and the air mass transport process can help us comprehend the characteristics of the target aerosols. Therefore, we conducted further analysis to examine the relationship between the PBL height and N_{INP}, and combined it with CWT analysis to explore the effect of transport on INPs at the sampling site.

At Changbai Mountain, changes in the PBL are also complicated by a variety of processes, such as orographic gravity waves, moist convection, and turbulent transport. Figure 5(a, b) shows the relationship between bio-INPs and the PBL height during the daytime. We found a positive correlation between PBL height and $N_{INP\text{-}bio}$ in the freezing temperature ranging from −25.0 ℃ to −15.0 ℃ (r = 0.4-0.8), especially significant spanning temperatures from −22.0 ℃ to −19.5 ℃ (r > 0.7, p < 0.05). However, the correlation was no longer observed when the freezing temperature above −15 ℃ (r < 0.5, p > 0.05). Notably, this correlation increased in the HLR when we excluded two outliers with exceptionally high $N_{INP\text{-}bio}$ values (as shown in Figure 5a, r increased to 0.77, p < 0.05). The two high values may be related to ocean and vegetation emissions, and they will be further discussed in the following paragraph. In brief, our findings suggest that an increase in the PBL height may cause a corresponding increase in $N_{INP\text{-}bio}$ in the clean mountaintop atmosphere. Moreover, based on the analysis of the air mass backward trajectory, our analysis revealed a significant increase in the height of the air mass backward trajectory as it moved through the southern mountainous regions (Figure S5). This phenomenon indicates that valley breezes promote the lifting of INPs from the bottom to the top of Changbai Mountain during the daytime.

The CWT analysis revealed the potential sources of bio-INPs, as shown in Figure 5(c, d). Ocean was identified as an important INPs source, as previous studies have reported that bubble bursting processes can release marine microorganisms (Burrows et al., 2013; Kwak et al., 2014; Mccluskey et al., 2018; Vergara-Temprado et al., 2017). Different ice nucleating entities can trigger droplets to freeze at various temperatures in the marine environment. For example, Wilson et al. (2015) found that the biogenic organic materials within the sea surface microlayer could induce droplet freezing under immersion mode, with a broad freezing temperature range of -7.0 °C to -35.0 °C. Laboratory experiments have further revealed that aerosols generated by phytoplankton are particularly effective at triggering ice nucleation at temperatures below −15.0 °C, with a notable increase in INP concentration within the range of −15.0 °C to −23.0 °C, which was related to the unique dynamic processes of phytoplankton bloom and growth (Brooks and Thornton, 2018; Mccluskey et al., 2017; Thornton et al., 2023; Wilbourn et al., 2020). Our study detected the high concentrations of bio-INPs in the LTR occurred in the Japan Sea (Figure 5d), implying that the air mass passing over the Japan Sea surface might have carried marine bio-INPs, contributing to their presence at our sampling site. In contrast, in the HTR, bio-INPs are mainly originate from the southern part of the Korean Peninsula. Previous studies demonstrated that vegetation contains a substantial density of microorganisms (10^6-10^7 cm^{-2}) and serves as a recognized reservoir of highly efficient biological INPs (Moore et al., 2021; Lindow and Brandl, 2003). These bio-INPs typically induce freezing at relatively warmer temperatures, which can be as high as −2~−5 °C (Schneider et al., 2021; Maki et al., 1974). South Korea has a large vegetation coverage area, as shown in Figure 1(a), with biological aerosols produced there able to reach our sampling site through long-distance transport.

The residence time of various biological particles in the atmosphere can range from less than a day to a few weeks, depending on their size and aerodynamic properties (Despres et al., 2012). The long-range transport of biological aerosols has been observed in previous studies. For example, abundant microbial components originating from the ocean or land have been found in the troposphere, even extending to the stratosphere and the middle layer (Burrows et al., 2009; Smith et al., 2013). High concentrations of microbial populations have also been identified in the background atmosphere during trans-Pacific intercontinental transport (Smith et al., 2013). In global transmission, microorganisms have been found to travel thousands of kilometers, with approximately 33%–68% originating in the ocean. This suggests that the ocean's bubble bursting processes play a significant role in the generation of biological aerosols. In addition, bio-INPs can attach to dust particles for long-distance transmission, with an adhesion rate that can even exceed 99.9% (Creamean et al., 2013; Yahya et al., 2019). This process can enable biological aerosol transmission over longer distances, with the ice nucleation activity of dust significantly enhanced (O'sullivan et al., 2016; Augustin-Bauditz et al., 2016). Notably, the above discussion in this study does not include the qualitative and quantitative analyses of biological particles with ice-nucleating activity. Although long-range transported bio-INPs were less prominent in our study, their contribution to the total INP concentration in the background atmosphere of northeastern Asia cannot be ignored.

In addition, a positive correlation was found between the PBL height and other org-INPs during the daytime, with significant correlations observed between −18.5 °C and −16.5 °C ($r > 0.7$, $p < 0.05$), as shown in Figure S4. However, when

the freezing temperatures greater than −15.0 °C, no correlation was observed between the PBL and $N_{\text{INP-other org}}$, suggesting that local sources may be an important source for other org-INPs. For the inorg-INPs, a weak correlation with the PBL height was observed at temperatures greater than −23.0 °C and was not statistically significant ($p > 0.05$). But at −24.5 °C and −24.0 °C, the correlation is more significant (r is 0.73 and 0.80, $p < 0.05$). The CWT simulation also indicated that high values of $N_{\text{INP-other org}}$ and $N_{INP\text{-}inorg}$ appeared in both local areas and adjacent Japan Sea regions (See Figure S6).

In summary, our findings suggest that valley breezes and the long-distance transport of air mass from the Japan Sea influence the diurnal cycles of INPs at Changbai Mountain. However, the impact of the PBL and valley breezes on the transport of inorg-INPs was found to be less significant than the contributions of bio-INPs and other org-INPs.

4 Conclusion

Measurements of INPs were carried out at the Changbai Mountain in northeastern Asia to explore the properties of INPs in the immersion freezing mode. Our results showed that N_{INP} spanned up to five orders of magnitude between 1.6×10^{-3} L^{-1} and 78.3 L^{-1} over the freezing temperature range from −29.0 °C to −5.5 °C, with these values corresponding to previously reported measurements for mountain sites.

The INPs that we observed primarily consisted of protein-based bio-INPs. The fractions of proteinaceous biological N_{INP} ($F_{\text{INP-bio}}$) accounted for 100% of N_{INP} above −11 °C, while showing a decreasing trend as the temperature decreased from −11.5 °C to −16.5 °C. The decreasing trend of $F_{\text{INP-bio}}$ suggested that the importance of bio-INPs decreases with temperature. However, $F_{\text{INP-bio}}$ increased from 0.8 to 0.9 as the temperature decreased from −16.5 °C to −21.5 °C, indicating that INPs have relatively high ice-nucleating activity in the low-temperature region (LTR, freezing temperature below T_{50}, -17.0 °C ~ -29.0 °C). When the temperature falls below -22.0 °C, $F_{\text{INP-bio}}$ exhibits a pronounced declining trend. We also found a significant positive correlation between biological INPs and both wind speed (WS) and Ca^{2+}, whereas there was only a weak positive correlation for biological INPs with isoprene and its oxidation products (isoprene × O_3). We speculate that the higher WS may facilitate the exposure of the local soil dust and bioaerosols containing bio-INPs to the atmosphere.

Our study also suggests that an increase in the planetary boundary layer (PBL) during the observation period may lead to a corresponding increase of diverse types of N_{INP} in the clean mountaintop atmosphere. During the daytime, valley breezes facilitate the orographic lifting of INPs from the bottom to the top of southern mountainous regions. However, for the high values of $N_{\text{INP-bio}}$, it may originate from long-distance transport from the Japan Sea and South Korea areas. We speculate that the oceanic and vegetation biogenic aerosols from these areas make significant contributions to the INPs at the top of the Changbai Mountain. Conversely, regional transport had a weaker effect on other org-INPs and inorg-INPs than bio-INPs, with larger contributions observed from local sources.

Our measurements in the high-altitude atmosphere above Northeast Asia indicate the predominant role of bio-INPs. However, our study has limitation in terms of dataset size. Further observational and modelling studies employing high-

resolution instruments are urgently needed to analyze the characteristics of INPs and their influence on ice crystal formation as well as the cloud properties in the high-altitude atmosphere.

Author contributions. Yue Sun analyzed data and wrote the paper. Likun Xue designed the research. Jiangshan Mu, Ye Shan, Mingxuan Liu, Yanbin Qi, Lingli Zhang and Yufei Wang conducted the field campaign. Lanxiadi Chen and Mingjin Tang provided guidance and assistance in the analysis of INPs samples. Yu Yang, Yanqiu Nie, Ping Liu, Can Cui and Ji Zhang helped with the interpretation of the results. Yujiao Zhu, Likun Xue, Xinfeng Wang and Wenxing Wang revised the original manuscript. All authors contributed toward improving the paper.

Competing interests. The authors declare that they have no conflict of interest.

Data availability. The datasets related to this work can be accessed via https://doi.org/10.17632/b9y6pfw39n.1 (Sun et al., 2023).

Acknowledgements. This work was funded by the National Natural Science Foundation of China (42075104, 41922051,42061160478). We are grateful to the staff of the Tianchi weather station for their logistical support and assistance during the field observations. We would also like to acknowledge the Global Data Assimilation System (GDAS) provided by the National Oceanic and Atmospheric Administration Air Resources Laboratory (NOAA ARL) for organizing and publishing the data, and the open-source software of MeteoInfo developed by Yaqiang Wang's team for the concentration-weighted trajectory (CWT) analysis.

References

Agresti, A. and Coull, B. A.: Approximate is better than "exact" for interval estimation of binomial proportions, Am. Stat., 52, 119-126, https://doi.org/10.2307/2685469, 1998.

Atkinson, J. D., Murray, B. J., Woodhouse, M. T., Whale, T. F., Baustian, K. J., Carslaw, K. S., Dobbie, S., O'Sullivan, D., and Malkin, T. L.: The importance of feldspar for ice nucleation by mineral dust in mixed-phase clouds, Nature, 498, 355-358, https://doi.org/10.1038/nature12278, 2013.

Augustin-Bauditz, S., Wex, H., Denjean, C., Hartmann, S., Schneider, J., Schmidt, S., Ebert, M., and Stratmann, F.: Laboratory-generated mixtures of mineral dust particles with biological substances: characterization of the particle mixing state and immersion freezing behavior, Atmos. Chem. Phys., 16, 5531-5543, https://doi.org/10.5194/acp-16-5531-2016, 2016.

Beall, C. M., Hill, T. C. J., DeMott, P. J., Köneman, T., Pikridas, M., Drewnick, F., Harder, H., Pöhlker, C., Lelieveld, J., Weber, B., Iakovides, M., Prokeš, R., Sciare, J., Andreae, M. O., Stokes, M. D., and Prather, K. A.: Ice-nucleating particles near two major dust source regions, Atmos Chem Phys, 22, 12607-12627, https://doi.org/10.5194/acp-22-12607-2022, 2022.

Bjordal, J., Storelvmo, T., Alterskjær, K., and Carlsen, T.: Equilibrium climate sensitivity above 5 °C plausible due to state-dependent cloud feedback, Nature Geoscience, 13, 718-721, https://doi.org/10.1038/s41561-020-00649-1, 2020.

Burrows, S. M., Elbert, W., Lawrence, M. G., and Pöschl, U.: Bacteria in the global atmosphere – Part 1: Review and synthesis of literature data for different ecosystems, Atmos. Chem. Phys., 9, 9263-9280, https://doi.org/10.5194/acp-9-9263-2009, 2009.

Burrows, S. M., Hoose, C., Poschl, U., and Lawrence, M. G.: Ice nuclei in marine air: biogenic particles or dust?, Atmos Chem Phys, 13, 245-267, 10.5194/acp-13-245-2013, 2013.

Chen, J., Wu, Z., Chen, J., Reicher, N., Fang, X., Rudich, Y., and Hu, M.: Size-resolved atmospheric ice-nucleating particles during East Asian dust events, Atmos Chem Phys, 21, 3491-3506, https://doi.org/10.5194/acp-21-3491-2021, 2021.

Chen, J., Wu, Z., Augustin-Bauditz, S., Grawe, S., Hartmann, M., Pei, X., Liu, Z., Ji, D., and Wex, H.: Ice-nucleating particle concentrations unaffected by urban air pollution in Beijing, China, Atmos Chem Phys, 18, 3523-3539, https://doi.org/10.5194/acp-18-3523-2018, 2018.

Chen, L., Peng, C., Chen, J., Chen, J., Gu, W., Jia, X., Wu, Z., Wang, Q., and Tang, M.: Effects of heterogeneous reaction with NO2 on ice nucleation activities of feldspar and Arizona Test Dust, J Environ Sci-China, 127, 210-221, https://doi.org/10.1016/j.jes.2022.04.034, 2023.

Chow, F. K., Wekker, S. F. D., and Snyder, B. J.: Mountain Weather Research and Mountain Weather Research and Forecasting: Recent Progress and Current Challenges, Springer Atmospheric Sciences, https://link.springer.com/book/10.1007/ 978-94-007-4098-3 (last access: 21 February 2022), 2013.

Conen, F., Yakutin, M. V., Yttri, K. E., and Hüglin, C.: Ice Nucleating Particle Concentrations Increase When Leaves Fall in Autumn, Atmosphere-Basel, 8, 202, https://doi.org/10.3390/atmos8100202, 2017.

Conen, F., Einbock, A., Mignani, C., and Hüglin, C.: Measurement report: Ice-nucleating particles active ≥ -15 °C in free tropospheric air over western Europe, Atmos. Chem. Phys., 22, 3433-3444, https://doi.org/10.5194/acp-22-3433-2022, 2022.

Cozic, J., Mertes, S., Verheggen, B., Cziczo, D. J., Gallavardin, S. J., Walter, S., Baltensperger, U., and Weingartner, E.: Black carbon enrichment in atmospheric ice particle residuals observed in lower tropospheric mixed phase clouds, J Geophys Res-Atmos, 113, 11, https://doi.org/10.1029/2007jd009266, 2008.

Creamean, J. M., Suski, K. J., Rosenfeld, D., Cazorla, A., DeMott, P. J., Sullivan, R. C., White, A. B., Ralph, F. M., Minnis, P., Comstock, J. M., Tomlinson, J. M., and Prather, K. A.: Dust and Biological Aerosols from the Sahara and Asia Influence Precipitation in the Western U.S, Science, 339, 1572-1578, https://doi.org/10.1126/science.1227279, 2013.

Cziczo, D. J., Froyd, K. D., Gallavardin, S. J., Moehler, O., Benz, S., Saathoff, H., and Murphy, D. M.: Deactivation of ice nuclei due to atmospherically relevant surface coatings, Environ Res Lett, 4, 9, https://doi.org/10.1088/1748-9326/4/4/044013, 2009.

Cziczo, D. J., Froyd, K. D., Hoose, C., Jensen, E. J., Diao, M. H., Zondlo, M. A., Smith, J. B., Twohy, C. H., and Murphy, D. M.: Clarifying the Dominant Sources and Mechanisms of Cirrus Cloud Formation, Science, 340, 1320-1324, https://doi.org/10.1126/science.1234145, 2013.

Daily, M. I., Tarn, M. D., Whale, T. F., and Murray, B. J.: An evaluation of the heat test for the ice-nucleating ability of minerals and biological material, Atmos. Meas. Tech., 15, 2635-2665, https://doi.org/10.5194/amt-15-2635-2022, 2022.

Demott, P. J.: An Exploratory Study of Ice Nucleation by Soot Aerosols, J Appl Meteorol, 29, 1072-1079, https://doi.org/10.1175/1520-0450(1990)029<1072:Aesoin>2.0.Co;2, 1990.

DeMott, P. J., Cziczo, D. J., Prenni, A. J., Murphy, D. M., Kreidenweis, S. M., Thomson, D. S., Borys, R., and Rogers, D. C.: Measurements of the concentration and composition of nuclei for cirrus formation, Proceedings of the National Academy of Sciences, 100, 14655-14660, https://doi.org/10.1073/pnas.2532677100, 2003.

DeMott, P. J., Prenni, A. J., Liu, X., Kreidenweis, S. M., Petters, M. D., Twohy, C. H., Richardson, M. S., Eidhammer, T., and Rogers, D. C.: Predicting global atmospheric ice nuclei distributions and their impacts on climate, P Natl Acad Sci USA, 107, 11217-11222, https://doi.org/10.1073/pnas.0910818107, 2010.

DeMott, P. J., Prenni, A. J., McMeeking, G. R., Sullivan, R. C., Petters, M. D., Tobo, Y., Niemand, M., Mohler, O., Snider, J. R., Wang, Z., and Kreidenweis, S. M.: Integrating laboratory and field data to quantify the immersion freezing ice nucleation activity of mineral dust particles, Atmos Chem Phys, 15, 393-409, https://doi.org/10.5194/acp-15-393-2015, 2015.

Despres, V. R., Huffman, J. A., Burrows, S. M., Hoose, C., Safatov, A. S., Buryak, G., Frohlich-Nowoisky, J., Elbert, W., Andreae, M. O., Poschl, U., and Jaenicke, R.: Primary biological aerosol particles in the atmosphere: a review, Tellus B, 64, 58, https://doi.org/10.3402/tellusb.v64i0.15598, 2012.

Freedman, M. A.: Potential Sites for Ice Nucleation on Aluminosilicate Clay Minerals and Related Materials, J. Phys. Chem. Lett., 6, 3850-3858, https://doi.org/10.1021/acs.jpclett.5b01326, 2015.

Gong, X., Radenz, M., Wex, H., Seifert, P., Ataei, F., Henning, S., Baars, H., Barja, B., Ansmann, A., and Stratmann, F.: Significant continental source of ice-nucleating particles at the tip of Chile's southernmost Patagonia region, Atmos Chem Phys, 22, 10505-10525, https://doi.org/10.5194/acp-2022-71, 2022.

Grawe, S., Augustin-Bauditz, S., Hartmann, S., Hellner, L., Pettersson, J. B. C., Prager, A., Stratmann, F., and Wex, H.: The immersion freezing behavior of ash particles from wood and brown coal burning, Atmos. Chem. Phys., 16, 13911-13928, https://doi.org/10.5194/acp-16-13911-2016, 2016.

Gute, E. and Abbatt, J. P. D.: Ice nucleating behavior of different tree pollen in the immersion mode, Atmospheric Environment, 231, 117488, https://doi.org/10.1016/j.atmosenv.2020.117488, 2020.

Hader, J. D., Wright, T. P., and Petters, M. D.: Contribution of pollen to atmospheric ice nuclei concentrations, Atmos. Chem. Phys., 14, 5433-5449, https://doi.org/10.5194/acp-14-5433-2014, 2014.

Hammer, S. E., Mertes, S., Schneider, J., Ebert, M., Kandler, K., and Weinbruch, S.: Composition of ice particle residuals in mixed-phase clouds at Jungfraujoch (Switzerland): enrichment and depletion of particle groups relative to total aerosol, Atmos Chem Phys, 18, 13987-14003, https://doi.org/10.5194/acp-18-13987-2018, 2018.

Hill, T. C. J., DeMott, P. J., Tobo, Y., Fröhlich-Nowoisky, J., Moffett, B. F., Franc, G. D., and Kreidenweis, S. M.: Sources of organic ice nucleating particles in soils, Atmos. Chem. Phys., 16, 7195-7211, https://doi.org/10.5194/acp-16-7195-2016, 2016.

Hoose, C. and Möhler, O.: Heterogeneous ice nucleation on atmospheric aerosols: a review of results from laboratory experiments, Atmos Chem Phys, 12, 9817-9854, https://doi.org/10.5194/acp-12-9817-2012, 2012.

Hodshire, A. L., Levin, E. J. T., Hallar, A. G., Rapp, C. N., Gilchrist, D. R., McCubbin, I., and McMeeking, G. R.: A High-Resolution Record of Ice Nuclei Concentrations Between -20 to -30 °C for Fall and Winter at Storm Peak Laboratory with the autonomous Continuous Flow Diffusion Chamber Ice Activation Spectrometer, Atmos. Meas. Tech. Discuss., 2022, 1-17, https://doi.org/10.5194/amt-2022-216, 2022.

Hsu, Y.-K., Holsen, T. M., and Hopke, P. K.: Comparison of hybrid receptor models to locate PCB sources in Chicago, Atmospheric Environment, 37, 545-562, https://doi.org/10.1016/S1352-2310(02)00886-5, 2003.

Huang, S., Hu, W., Chen, J., Wu, Z., Zhang, D., and Fu, P.: Overview of biological ice nucleating particles in the atmosphere, Environment International, 146, 106197, https://doi.org/10.1016/j.envint.2020.106197, 2021.

Hummel, M., Hoose, C., Pummer, B., Schaupp, C., Frohlich-Nowoisky, J., and Mohler, O.: Simulating the influence of primary biological aerosol particles on clouds by heterogeneous ice nucleation, Atmos Chem Phys, 18, 15437-15450, https://doi.org/10.5194/acp-18-15437-2018, 2018.

Iannone, R., Chernoff, D. I., Pringle, A., Martin, S. T., and Bertram, A. K.: The ice nucleation ability of one of the most abundant types of fungal spores found in the atmosphere, Atmos Chem Phys, 11, 1191-1201, https://doi.org/10.5194/acp-11-1191-2011, 2011.

Lau, K. M. and Wu, H. T.: Warm rain processes over tropical oceans and climate implications, Geophys Res Lett, 30, 5, https://doi.org/10.1029/2003gl018567, 2003.

Jiang, H., Yin, Y., Su, H., Shan, Y. P., and Gao, R. J.: The characteristics of atmospheric ice nuclei measured at the top of Huangshan (the Yellow Mountains) in Southeast China using a newly built static vacuum water vapor diffusion chamber, Atmos Res, 153, 200-208, https://doi.org/10.1016/j.atmosres.2014.08.015, 2015.

Jiang, H., Yin, Y., Chen, K., Chen, Q., He, C., and Sun, L.: The measurement of ice nucleating particles at Tai'an city in East China, Atmos Res, 232, 9, https://doi.org/10.1016/j.atmosres.2019.104684, 2020.

Jiang, H., Yin, Y., Yang, L., Yang, S. Z., Su, H., and Chen, K.: The Characteristics of Atmospheric Ice Nuclei Measured at Different Altitudes in the Huangshan Mountains in Southeast China, Adv. Atmos. Sci., 31, 396-406, https://doi.org/10.1007/s00376-013-3048-5, 2014.

Jin, Y. H., Zhang, Y. J., Xu, J. W., Tao, Y., He, H. S., Guo, M., Wang, A. L., Liu, Y. X., and Niu, L. P.: Comparative Assessment of Tundra Vegetation Changes Between North and Southwest Slopes of Changbai Mountains, China, in Response to Global Warming, Chin. Geogr. Sci., 28, 665-679, https://doi.org/10.1007/s11769-018-0978-y, 2018.

Joly, M., Amato, P., Deguillaume, L., Monier, M., Hoose, C., and Delort, A. M.: Quantification of ice nuclei active at near 0 °C temperatures in low-altitude clouds at the Puy de Dôme atmospheric station, Atmos. Chem. Phys., 14, 8185-8195, https://doi.org/10.5194/acp-14-8185-2014, 2014.

Jung, S., Tiwari, M. K., and Poulikakos, D.: Frost halos from supercooled water droplets, P Natl Acad Sci USA, 109, 16073-16078, https://doi.org/10.1073/pnas.1206121109, 2012.

Kanji, Z. A. and Abbattt, J. P. D.: Ice Nucleation onto Arizona Test Dust at Cirrus Temperatures: Effect of Temperature and Aerosol Size on Onset Relative Humidity, J Phys Chem A, 114, 935-941, https://doi.org/10.1021/jp908661m, 2010.

Kanji, Z. A., Ladino, L. A., Wex, H., Boose, Y., Burkert-Kohn, M., Cziczo, D. J., and Krämer, M.: Overview of Ice Nucleating Particles, Meteorological Monographs, 58, 1.1-1.33, https://doi.org/10.1175/amsmonographs-d-16-0006.1, 2017.

Knopf, D. A., Wang, B., Laskin, A., Moffet, R. C., and Gilles, M. K.: Heterogeneous nucleation of ice on anthropogenic organic particles collected in Mexico City, Geophys Res Lett, 37, 5, https://doi.org/10.1029/2010gl043362, 2010.

Koop, T., Luo, B., Tsias, A., and Peter, T.: Water activity as the determinant for homogeneous ice nucleation in aqueous solutions, Nature, 406, 611-614, https://doi.org/10.1038/35020537, 2000.

Kunert, A. T., Pöhlker, M. L., Tang, K., Krevert, C. S., Wieder, C., Speth, K. R., Hanson, L. E., Morris, C. E., Schmale Iii, D. G., Pöschl, U., and Fröhlich-Nowoisky, J.: Macromolecular fungal ice nuclei in Fusarium: effects of physical and chemical processing, Biogeosciences, 16, 4647-4659, https://doi.org/10.5194/bg-16-4647-2019, 2019.

Kwak, J. H., Lee, S. H., Hwang, J., Suh, Y. S., Park, H. J., Chang, K. I., Kim, K. R., and Kang, C. K.: Summer primary productivity and phytoplankton community composition driven by different hydrographic structures in the East/Japan Sea and the Western Subarctic Pacific, J. Geophys. Res.-Oceans, 119, 4505-4519, https://doi.org/10.1002/2014jc009874, 2014.

Levin, E. J. T., McMeeking, G. R., DeMott, P. J., McCluskey, C. S., Carrico, C. M., Nakao, S., Jayarathne, T., Stone, E. A., Stockwell, C. E., Yokelson, R. J., and Kreidenweis, S. M.: Ice-nucleating particle emissions from biomass combustion and the potential importance of soot aerosol, J Geophys Res-Atmos, 121, 5888-5903, https://doi.org/10.1002/2016jd024879, 2016.

Lindow, S. E. and Brandl, M. T.: Microbiology of the Phyllosphere, Appl. Environ. Microbiol., 69, 1875-1883, https://doi.org/10.1128/AEM.69.4.1875-1883.2003, 2003.

Lu, Z. D., Du, P. R., Du, R., Liang, Z. M., Qin, S. S., Li, Z. M., and Wang, Y. L.: The Diversity and Role of Bacterial Ice Nuclei in Rainwater from Mountain Sites in China, Aerosol Air Qual Res, 16, 640-652, https://doi.org/10.4209/aaqr.2015.05.0315, 2016.

Mahrt, F., Marcolli, C., David, R. O., Gronquist, P., Meier, E. J. B., Lohmann, U., and Kanji, Z. A.: Ice nucleation abilities of soot particles determined with the Horizontal Ice Nucleation Chamber, Atmos Chem Phys, 18, 13363-13392, https://doi.org/10.5194/acp-18-13363-2018, 2018.

Maki, L. R., Galyan, E. L., Changchi.Mm, and Caldwell, D. R.: Ice Nucleation Induced by Pseudomonas syringae, Applied Microbiology, 28, 456-459, https://doi.org/10.1128/aem.28.3.456-459.1974, 1974.

McCluskey, C. S., Hill, T. C. J., Malfatti, F., Sultana, C. M., Lee, C., Santander, M. V., Beall, C. M., Moore, K. A., Cornwell, G. C., Collins, D. B., Prather, K. A., Jayarathne, T., Stone, E. A., Azam, F., Kreidenweis, S. M., and DeMott, P. J.: A Dynamic Link between Ice Nucleating Particles Released in Nascent Sea Spray Aerosol and Oceanic Biological Activity during Two Mesocosm Experiments, J Atmos Sci, 74, 151-166, 10.1175/jas-d-16-0087.1, 2017.

McCluskey, C. S., Ovadnevaite, J., Rinaldi, M., Atkinson, J., Belosi, F., Ceburnis, D., Marullo, S., Hill, T. C. J., Lohmann, U., Kanji, Z. A., O'Dowd, C., Kreidenweis, S. M., and DeMott, P. J.: Marine and Terrestrial Organic Ice-Nucleating Particles in Pristine Marine to Continentally Influenced Northeast Atlantic Air Masses, J Geophys Res-Atmos, 123, 6196-6212, https://doi.org/10.1029/2017jd028033, 2018.

Moffett, B. F., Getti, G., Henderson-Begg, S. K., and Hill, T. C. J.: Ubiquity of ice nucleation in lichen — possible atmospheric implications, Lindbergia, 3, 39-43, https://doi.org/10.25227/linbg.01070, 2015.

Moore, R. A., Bomar, C., Kobziar, L. N., and Christner, B. C.: Wildland fire as an atmospheric source of viable microbial aerosols and biological ice nucleating particles, The ISME Journal, 15, 461-472, https://doi.org/10.1038/s41396-020-00788-8, 2021.

Mulmenstadt, J., Sourdeval, O., Delanoe, J., and Quaas, J.: Frequency of occurrence of rain from liquid-, mixed-, and ice-phase clouds derived from A-Train satellite retrievals, Geophys Res Lett, 42, 6502-6509, https://doi.org/10.1002/2015gl064604, 2015.

Murray, B. J., O'Sullivan, D., Atkinson, J. D., and Webb, M. E.: Ice nucleation by particles immersed in supercooled cloud droplets, Chem. Soc. Rev., 41, 6519-6554, https://doi.org/10.1039/c2cs35200a, 2012.

Murray, B. J., Broadley, S. L., Wilson, T. W., Bull, S. J., Wills, R. H., Christenson, H. K., and Murray, E. J.: Kinetics of the homogeneous freezing of water, Phys Chem Chem Phys, 12, 10380-10387, https://doi.org/10.1039/C003297B, 2010.

Nichman, L., Wolf, M., Davidovits, P., Onasch, T. B., Zhang, Y., Worsnop, D. R., Bhandari, J., Mazzoleni, C., and Cziczo, D. J.: Laboratory study of the heterogeneous ice nucleation on black-carbon-containing aerosol, Atmos. Chem. Phys., 19, 12175-12194, https://doi.org/10.5194/acp-19-12175-2019, 2019.

O'Sullivan, D., Murray, B. J., Malkin, T. L., Whale, T. F., Umo, N. S., Atkinson, J. D., Price, H. C., Baustian, K. J., Browse, J., and Webb, M. E.: Ice nucleation by fertile soil dusts: relative importance of mineral and biogenic components, Atmos. Chem. Phys., https://doi.org/14, 1853-1867, 10.5194/acp-14-1853-2014, 2014.

O'Sullivan, D., Murray, B. J., Ross, J. F., and Webb, M. E.: The adsorption of fungal ice-nucleating proteins on mineral dusts: a terrestrial reservoir of atmospheric ice-nucleating particles, Atmos. Chem. Phys., 16, 7879-7887, https://doi.org/10.5194/acp-16-7879-2016, 2016.

O'Sullivan, D., Adams, M. P., Tarn, M. D., Harrison, A. D., Vergara-Temprado, J., Porter, G. C. E., Holden, M. A., Sanchez-Marroquin, A., Carotenuto, F., Whale, T. F., McQuaid, J. B., Walshaw, R., Hedges, D. H. P., Burke, I. T., Cui, Z., and Murray, B. J.: Contributions of biogenic material to the atmospheric ice-nucleating particle population in North Western Europe, Sci Rep, 8, 13821, https://doi.org/10.1038/s41598-018-31981-7, 2018.

Petters, M. D. and Wright, T. P.: Revisiting ice nucleation from precipitation samples, Geophys Res Lett, 42, 8758-8766, https://doi.org/10.1002/2015GL065733, 2015.

Phelps, P., Giddings, T. H., Prochoda, M., and Fall, R.: Release of cell-free ice nuclei by Erwinia herbicola, J. Bacteriol., 167, 496-502, https://doi.org/10.1128/jb.167.2.496-502.1986, 1986.

Phillips, V. T. J., Donner, L. J., and Garner, S. T.: Nucleation Processes in Deep Convection Simulated by a Cloud-System-Resolving Model with Double-Moment Bulk Microphysics, J Atmos Sci, 64, 738-761, https://doi.org/10.1175/jas3869.1, 2007.

Pratt, K. A., DeMott, P. J., French, J. R., Wang, Z., Westphal, D. L., Heymsfield, A. J., Twohy, C. H., Prenni, A. J., and Prather, K. A.: In situ detection of biological particles in cloud ice-crystals, Nature Geoscience, 2, 397-400, https://doi.org/10.1038/ngeo521, 2009.

Pummer, B. G., Bauer, H., Bernardi, J., Bleicher, S., and Grothe, H.: Suspendable macromolecules are responsible for ice nucleation activity of birch and conifer pollen, Atmos Chem Phys, 12, 2541-2550, https://doi.org/10.5194/acp-12-2541-2012, 2012.

Rinaldi, M., Santachiara, G., Nicosia, A., Piazza, M., Decesari, S., Gilardoni, S., Paglione, M., Cristofanelli, P., Marinoni, A., Bonasoni, P., and Belosi, F.: Atmospheric Ice Nucleating Particle measurements at the high mountain observatory Mt. Cimone (2165 m a.s.l., Italy), Atmospheric Environment, 171, 173-180, https://doi.org/10.1016/j.atmosenv.2017.10.027, 2017.

Rosenfeld, D. and Woodley, W. L.: Deep convective clouds with sustained supercooled liquid water down to - 37.5 °C, Nature, 405, 440-442, https://doi.org/10.1038/35013030, 2000.

Roudsari, G., Pakarinen, O. H., Reischl, B., and Vehkamäki, H.: Atomistic and coarse-grained simulations reveal increased ice nucleation activity on silver iodide surfaces in slit and wedge geometries, Atmos. Chem. Phys., 22, 10099-10114, https://doi.org/10.5194/acp-22-10099-2022, 2022.

Sassen, K. and Khvorostyanov, V. I.: Cloud effects from boreal forest fire smoke: evidence for ice nucleation from polarization lidar data and cloud model simulations, Environ Res Lett, 3, 12, https://doi.org/10.1088/1748-9326/3/2/025006, 2008.

Schill, G. P., DeMott, P. J., Emerson, E. W., Rauker, A. M. C., Kodros, J. K., Suski, K. J., Hill, T. C. J., Levin, E. J. T., Pierce, J. R., Farmer, D. K., and Kreidenweis, S. M.: The contribution of black carbon to global ice nucleating particle concentrations relevant to mixed-phase clouds, P Natl Acad Sci USA, 117, 22705-22711, https://doi.org/10.1073/pnas.2001674117, 2020.

Schneider, J., Höhler, K., Heikkilä, P., Keskinen, J., Bertozzi, B., Bogert, P., Schorr, T., Umo, N. S., Vogel, F., Brasseur, Z., Wu, Y., Hakala, S., Duplissy, J., Moisseev, D., Kulmala, M., Adams, M. P., Murray, B. J., Korhonen, K., Hao, L.,

Thomson, E. S., Castarède, D., Leisner, T., Petäjä, T., and Möhler, O.: The seasonal cycle of ice-nucleating particles linked to the abundance of biogenic aerosol in boreal forests, Atmos. Chem. Phys., 21, 3899-3918, https://doi.org/10.5194/acp-21-3899-2021, 2021.

Schrod, J., Weber, D., Drucke, J., Keleshis, C., Pikridas, M., Ebert, M., Cvetkovic, B., Nickovic, S., Marinou, E., Baars, H., Ansmann, A., Vrekoussis, M., Mihalopoulos, N., Sciare, J., Curtius, J., and Bingemer, H. G.: Ice nucleating particles over the Eastern Mediterranean measured by unmanned aircraft systems, Atmos Chem Phys, 17, 4817-4835, https://doi.org/10.5194/acp-17-4817-2017, 2017.

Smith, D. J., Timonen, H. J., Jaffe, D. A., Griffin, D. W., Birmele, M. N., Perry, K. D., Ward, P. D., and Roberts, M. S.: Intercontinental Dispersal of Bacteria and Archaea by Transpacific Winds, Appl. Environ. Microbiol., 79, 1134-1139, https://doi.org/10.1128/AEM.03029-12, 2013.

Stein, A. F., Draxler, R. R., Rolph, G. D., Stunder, B. J. B., Cohen, M. D., and Ngan, F.: NOAA's HYSPLIT Atmospheric Transport and Dispersion Modeling System, Bulletin of the American Meteorological Society, 96, 2059-2077, https://doi.org/10.1175/bams-d-14-00110.1, 2015.

Sugita, M., Asanuma, J., Tsujimura, M., Mariko, S., Lu, M., Kimura, F., Azzaya, D., and Adyasuren, T.: An overview of the rangelands atmosphere–hydrosphere–biosphere interaction study experiment in northeastern Asia (RAISE), J Hydrol, 333, 3-20, https://doi.org/10.1016/j.jhydrol.2006.07.032, 2007.

Suski, K. J., Hill, T. C. J., Levin, E. J. T., Miller, A., DeMott, P. J., and Kreidenweis, S. M.: Agricultural harvesting emissions of ice-nucleating particles, Atmos. Chem. Phys., 18, 13755-13771, https://doi.org/10.5194/acp-18-13755-2018, 2018.

Tang, M. J., Chen, J., and Wu, Z.: Ice nucleating particles in the troposphere: Progresses, challenges and opportunities, Atmospheric Environment, 192, 206-208, https://doi.org/10.1016/j.atmosenv.2018.09.004, 2018.

Tang, M. J., Cziczo, D. J., and Grassian, V. H.: Interactions of Water with Mineral Dust Aerosol: Water Adsorption, Hygroscopicity, Cloud Condensation, and Ice Nucleation, Chem Rev, 116, 4205-4259, https://doi.org/10.1021/acs.chemrev.5b00529, 2016.

Testa, B., Hill, T. C. J., Marsden, N. A., Barry, K. R., Hume, C. C., Bian, Q. J., Uetake, J., Hare, H., Perkins, R. J., Mohler, O., Kreidenweis, S. M., and DeMott, P. J.: Ice Nucleating Particle Connections to Regional Argentinian Land Surface Emissions and Weather During the Cloud, Aerosol, and Complex Terrain Interactions Experiment, J Geophys Res-Atmos, 126, 26, https://doi.org/10.1029/2021jd035186, 2021.

Thornton, D. C. O., Brooks, S. D., Wilbourn, E. K., Mirrielees, J., Alsante, A. N., Gold-Bouchot, G., Whitesell, A., and Kiana McFadden, K.: Production of aerosol containing ice nucleating particles (INPs) by fast growing phytoplankton, Atmos. Chem. Phys. Discuss., 2023, 1-30, https://doi.org/10.5194/acp-2022-806, 2023.

Tobo, Y., Prenni, A. J., DeMott, P. J., Huffman, J. A., McCluskey, C. S., Tian, G. X., Pohlker, C., Poschl, U., and Kreidenweis, S. M.: Biological aerosol particles as a key determinant of ice nuclei populations in a forest ecosystem, J Geophys Res-Atmos, 118, 10100-10110, https://doi.org/10.1002/jgrd.50801, 2013.

Vali, G.: Quantitative Evaluation of Experimental Results an the Heterogeneous Freezing Nucleation of Supercooled Liquids, Journal of Atmospheric Sciences, 28, 402-409, https://doi.org/10.1175/1520-0469(1971)028<0402:Qeoera>2.0.Co;2, 1971.

Vali, G., DeMott, P. J., Mohler, O., and Whale, T. F.: Technical Note: A proposal for ice nucleation terminology, Atmos Chem Phys, 15, 10263-10270, https://doi.org/10.5194/acp-15-10263-2015, 2015.

Vergara-Temprado, J., Murray, B. J., Wilson, T. W., O'Sullivan, D., Browse, J., Pringle, K. J., Ardon-Dryer, K., Bertram, A. K., Burrows, S. M., Ceburnis, D., DeMott, P. J., Mason, R. H., O'Dowd, C. D., Rinaldi, M., and Carslaw, K. S.: Contribution of feldspar and marine organic aerosols to global ice nucleating particle concentrations, Atmos. Chem. Phys., 17, 3637-3658, https://doi.org/10.5194/acp-17-3637-2017, 2017.

Wang, Z. W., Gallet, J. C., Pedersen, C. A., Zhang, X. S., Ström, J., and Ci, Z. J.: Elemental carbon in snow at Changbai Mountain, northeastern China: concentrations, scavenging ratios, and dry deposition velocities, Atmos. Chem. Phys., 14, 629-640, https://doi.org/10.5194/acp-14-629-2014, 2014.

Welti, A., Müller, K., Fleming, Z. L., and Stratmann, F.: Concentration and variability of ice nuclei in the subtropical maritime boundary layer, Atmos. Chem. Phys., 18, 5307-5320, 10.5194/acp-18-5307-2018, 2018.

Wieder, J., Mignani, C., Schär, M., Roth, L., Sprenger, M., Henneberger, J., Lohmann, U., Brunner, C., and Kanji, Z. A.: Unveiling atmospheric transport and mixing mechanisms of ice-nucleating particles over the Alps, Atmos Chem Phys, 22, 3111-3130, https://doi.org/10.5194/acp-22-3111-2022, 2022.

Wilson, T. W., Ladino, L. A., Alpert, P. A., Breckels, M. N., Brooks, I. M., Browse, J., Burrows, S. M., Carslaw, K. S., Huffman, J. A., Judd, C., Kilthau, W. P., Mason, R. H., McFiggans, G., Miller, L. A., Nájera, J. J., Polishchuk, E., Rae, S., Schiller, C. L., Si, M., Temprado, J. V., Whale, T. F., Wong, J. P. S., Wurl, O., Yakobi-Hancock, J. D., Abbatt, J. P. D., Aller, J. Y., Bertram, A. K., Knopf, D. A., and Murray, B. J.: A marine biogenic source of atmospheric ice-nucleating particles, Nature, 525, 234-238, https://doi.org/10.1038/nature14986, 2015.

Wolf, M. J., Zhang, Y., Zawadowicz, M. A., Goodell, M., Froyd, K., Freney, E., Sellegri, K., Rosch, M., Cui, T. Q., Winter, M., Lacher, L., Axisa, D., DeMott, P. J., Levin, E. J. T., Gute, E., Abbatt, J., Koss, A., Kroll, J. H., Surratt, J. D., and Cziczo, D. J.: A biogenic secondary organic aerosol source of cirrus ice nucleating particles, Nat. Commun., 11, 9, https://doi.org/10.1038/s41467-020-18424-6, 2020.

Yahya, R. Z., Arrieta, J. M., Cusack, M., and Duarte, C. M.: Airborne Prokaryote and Virus Abundance Over the Red Sea, Front. Microbiol., 10, 10, https://doi.org/10.3389/fmicb.2019.01112, 2019.

Zhang, P., Wu, Z., and Jin, R.: How can the winter North Atlantic Oscillation influence the early summer precipitation in Northeast Asia: effect of the Arctic sea ice, Clim Dynam, 56, 1989-2005, https://doi.org/10.1007/s00382-020-05570-2, 2021.

Zhao, X., Kim, S.-K., Zhu, W., Kannan, N., and Li, D.: Long-range atmospheric transport and the distribution of polycyclic aromatic hydrocarbons in Changbai Mountain, Chemosphere, 119, 289-294, https://doi.org/10.1016/j.chemosphere.2014.06.005, 2015.

Zhou, C., Zelinka, M. D., and Klein, S. A.: Impact of decadal cloud variations on the Earth's energy budget, Nature Geoscience, 9, 871-874, https://doi.org/10.1038/ngeo2828, 2016.

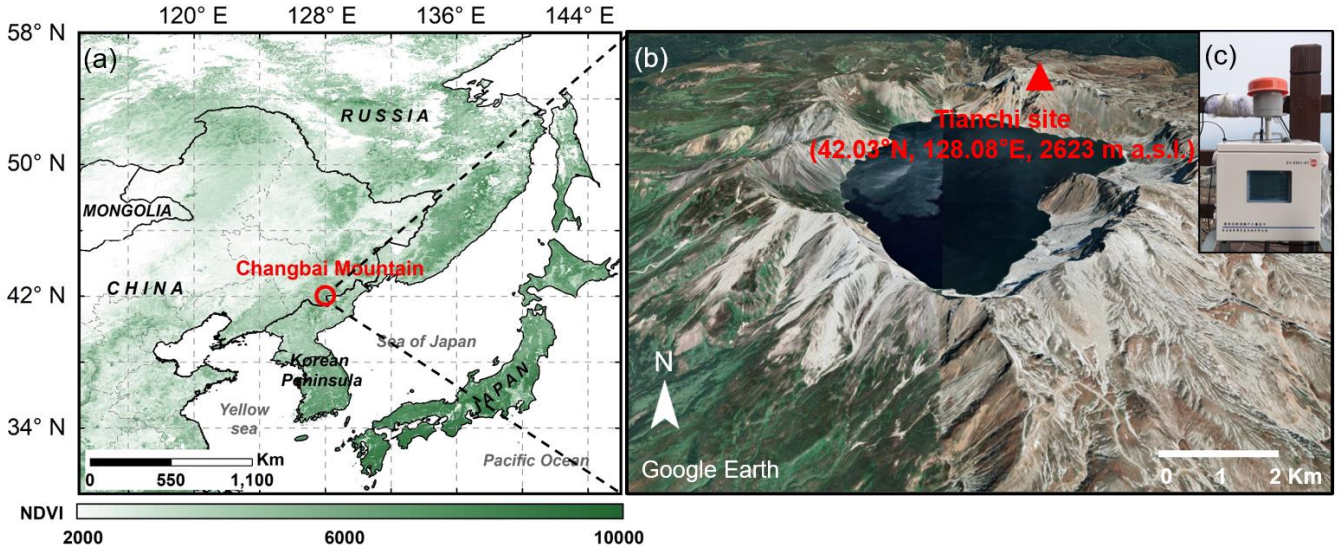

Figure 1. Geographical maps showing the location of Changbai Mountain. (a) This map is color-coded according to the normalized difference vegetation index (NDVI) in 2015, which was downloaded from the Geospatial Data Cloud (https://www.gscloud.cn/search). (b) This map shows the three-dimensional shape of the sampling site, which was obtained from Google Earth. (c) The ice nuclei sampler (The TH-150D medium flow sampler, Wuhan Tianhong Corporation, China).

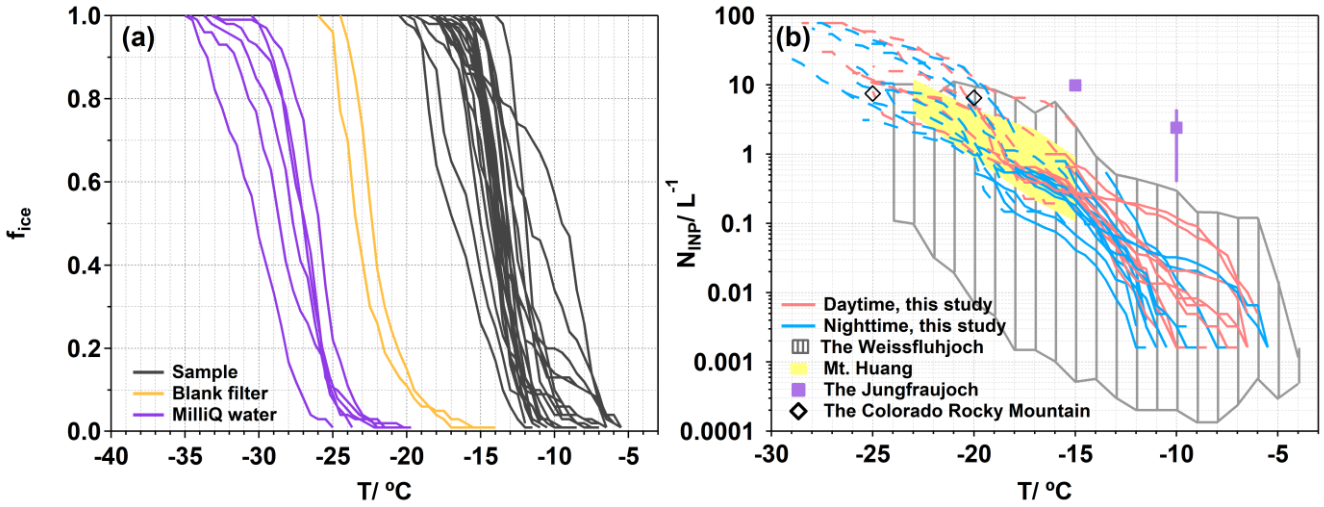

Figure 2. Frozen fractions (f_{ice}) and concentrations of INPs (N_{INP}) as functions of temperature. (a) The f_{ice} of collected samples measured by GIGINA is shown by the black curves, and presented together with blank filters (orange curves) and MilliQ water (purple curves) as background signals. (b) N_{INP} was measured during the daytime and nighttime. The dark gray shaded area represents the upper and lower limits of N_{INP} over the Weissfluhjoch (2693 m a.s.l.) (Wieder et al., 2022). The yellow shaded area represents the atmospheric N_{INP} ranges at Mt. Huang (1840 m a.s.l) (Jiang et al., 2015). The purple square represents the median N_{INP} at −15 °C and −10 °C in the Jungfraujoch (3580 m a.s.l.) (Conen et al., 2022). And the black rhombus represents the median N_{INP} at −25 °C and −20 °C at the Storm Peak Laboratory in the northwestern Colorado Rocky Mountains (3220 m a.s.l.) (Hodshire et al., 2022).

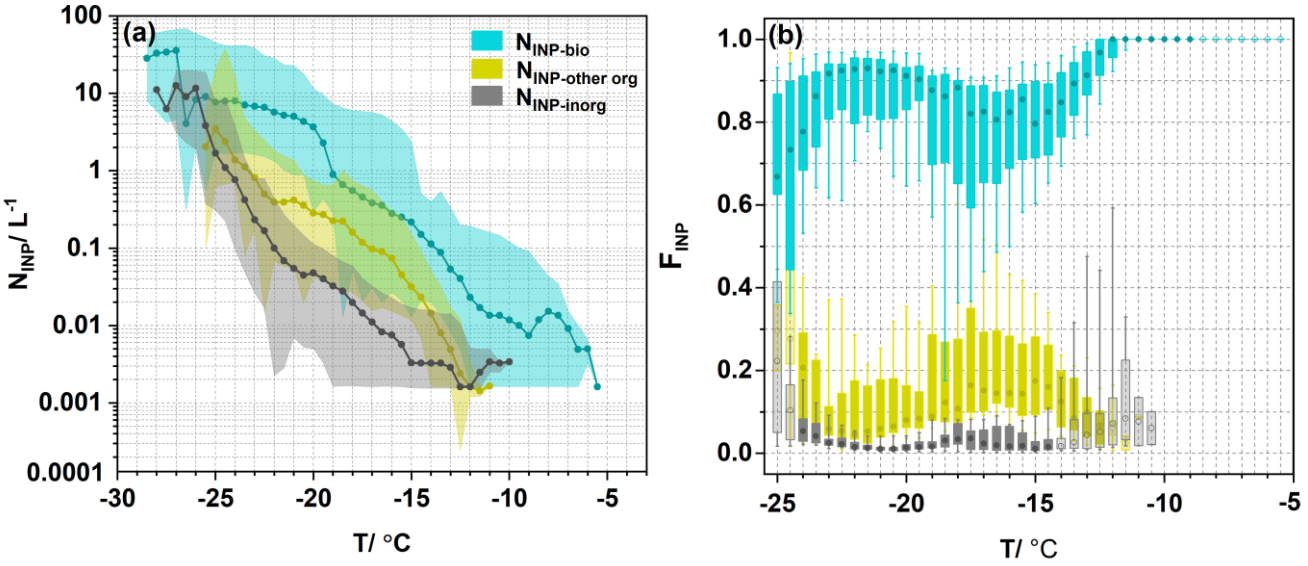

Figure 3. N_{INP} **for different types of INPs and their fractions as functions of temperature. (a) The INPs spectra of biological INPs (**$N_{INP\text{-}bio}$**, blue dots), other organic INPs (**$N_{INP\text{-}other\ org}$**, yellow dots), and inorganic INPs (**$N_{INP\text{-}inorg}$**, gray dots). The point plot represents the median value. The shadow area represents the maximum and minimum value. (b) Boxplot of fractions of bio-INPs (**$F_{INP\text{-}bio}$**, blue boxplot), other org-INPs (**$F_{INP\text{-}other\ org}$**, yellow boxplot), and inorganic INPs (**$F_{INP\text{-}inorg}$**, gray boxplot) as functions of temperature. The upper and lower extents of the boxes represent the 75th and 25th percentiles, respectively, while the whiskers indicate the 10th and 90th values. The circle in each boxplot represents the median value. The light-colored boxes indicate that the number of data points is less than half (the sample number is less than 11) of all samples at each temperature.**

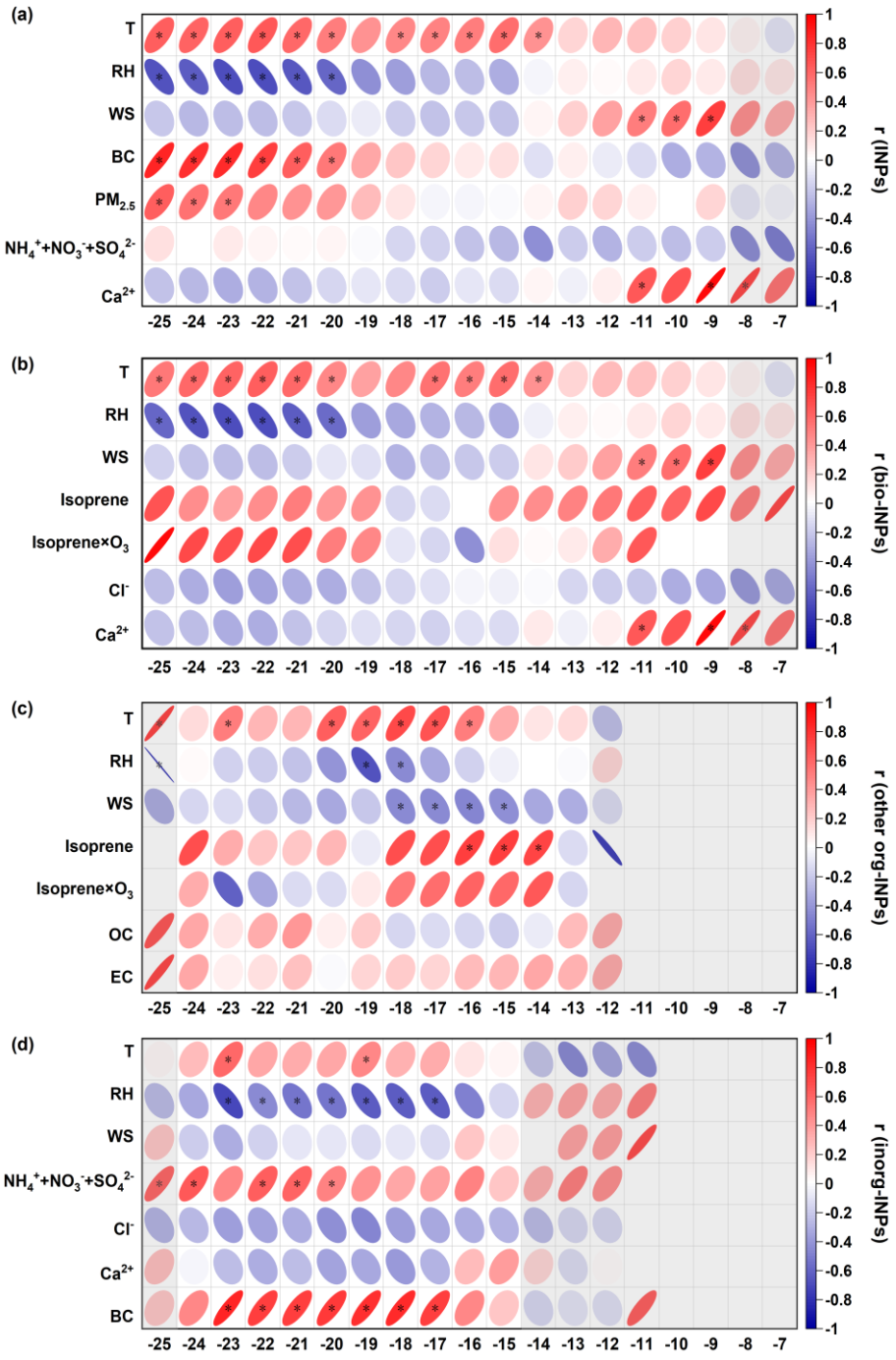

Figure 4. Correlation analysis between (a) N_{INP}, (b) $N_{INP\text{-}bio}$, (c) $N_{INP\text{-}other\ org}$, (d) $N_{INP\text{-}inorg}$, and meteorological parameters, chemical compositions, as functions of temperature. The *r* denotes the Pearson correlation coefficients. The asterisk indicates $p < 0.05$, while the shades indicate that the number of data points is less than half of all samples at each temperature.

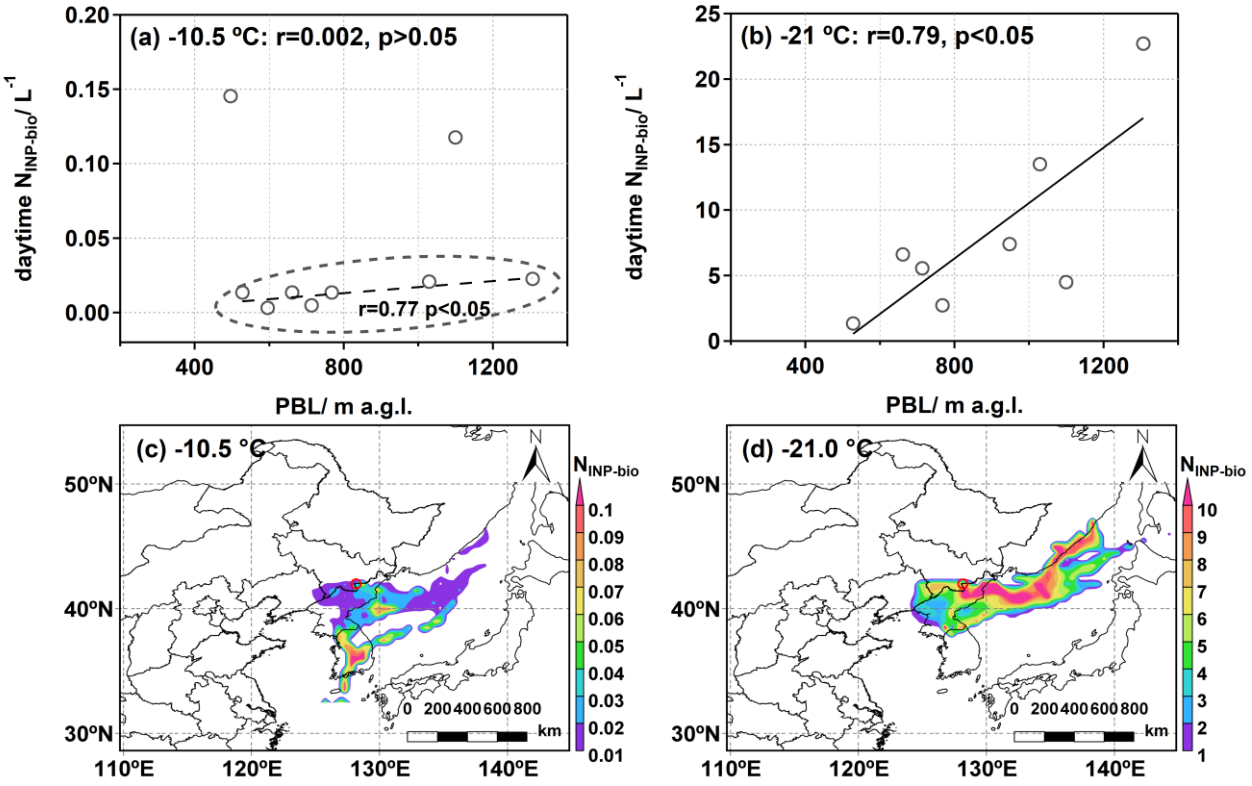

Figure 5. (a-b) Relationship between $N_{INP-bio}$ and average PBL height during the daytime (8:00–17:00 LT) at freezing temperature of −10.5 °C and −21.0 °C. The *r* denotes the Pearson correlation coefficients. (c-d) The concentration-weighted trajectory (CWT) analysis for the distribution of $N_{INP-bio}$ at −10.5 °C and −21.0 °C during the measurement. The red circle represents the Tianchi site.